AD_____

Award Number: W81XWH-06-1-0207

TITLE: Biological Impact of Senescence Induction in Prostate Cancer Therapy

PRINCIPAL INVESTIGATOR: David F. Jarrard, M.D.

CONTRACTING ORGANIZATION: University of Wisconsin
Madison, WI 53792

REPORT DATE: January 2009

TYPE OF REPORT: Annual

PREPARED FOR: U.S. Army Medical Research and Materiel Command
Fort Detrick, Maryland 21702-5012

REPORT DOCUMENTATION PAGE

Form Approved
OMB No. 0704-0188

1. REPORT DATE *(DD-MM-YYYY)*	**2. REPORT TYPE**	**3. DATES COVERED** *(From - To)*
01-01-2009	Annual	15 DEC 2007 - 14 DEC 2008

4. TITLE AND SUBTITLE

Biological Impact of Senescence Induction in Prostate Cancer

5a. CONTRACT NUMBER

5b. GRANT NUMBER
W81XWH-06-1-0207

5c. PROGRAM ELEMENT NUMBER

6. AUTHOR(S)
David F. Jarrard, M.D.

E-Mail: jarrard@surgery.wisc.edu

5d. PROJECT NUMBER

5e. TASK NUMBER

5f. WORK UNIT NUMBER

7. PERFORMING ORGANIZATION NAME(S) AND ADDRESS(ES)

Univeraity of Wisconsin
Madison, WI 53792

8. PERFORMING ORGANIZATION REPORT NUMBER

9. SPONSORING / MONITORING AGENCY NAME(S) AND ADDRESS(ES)
U.S. Army Medical Research and Materiel Command
Fort Detrick, Maryland 21702-5012

10. SPONSOR/MONITOR'S ACRONYM(S)

11. SPONSOR/MONITOR'S REPORT NUMBER(S)

12. DISTRIBUTION / AVAILABILITY STATEMENT
Approved for Public Release; Distribution Unlimited

13. SUPPLEMENTARY NOTES

14. ABSTRACT
Recently, it has been recognized that a distinct mechanism of terminal proliferation arrest after chemotherapy involves the reactivation of senescence. However, whether this phenotype occurs in vivo is unclear, as is the biological impact of senescence induction. We have previously identified pathways and genes involved in human senescence that may serve as senescence markers, and have demonstrated that senescence occurs in prostate cancer cell lines after chemotherapy. In this proposal, we will: a) determine whether senescent tumor cells alter the proliferation and invasion of surrounding prostate cancer cells in vitro and in vivo, b) assess for and augment senescence in prostate cancer xenograft models and human tumors, and c) identify novel small molecules that induce senescence in prostate cancer cells. Both in vitro and in vivo approaches using human prostate cancer cells will be utilized to identify and determine the mechanisms underlying senescence. With this data, our understanding of cellular senescence will undergo a quantum leap and permit the translation of this entity both as a marker of response and for directing therapy..

15. SUBJECT TERMS
Androgen receptor, prostate cancer, DNA methylation

16. SECURITY CLASSIFICATION OF:			**17. LIMITATION OF ABSTRACT**	**18. NUMBER OF PAGES**	**19a. NAME OF RESPONSIBLE PERSON**
a. REPORT	**b. ABSTRACT**	**c. THIS PAGE**			USAMRMC
U	U	U	UU	48	**19b. TELEPHONE NUMBER** *(include area code)*

Table of Contents

Update and Report

Introduction:

Senescence is an irreversible process that limits the lifespan of normal cells. It is believed to represent a tumor-suppression mechanism that is lost during neoplastic transformation. The induction of accelerated senescence, like other damage responses such as apoptosis, is a programmed response to a carcinogenic or biological insult involving multiple molecular pathways. It has recently been appreciated that senescence may also be a cytostatic response *reactivated* in tumor cells in response to chemotherapeutic agents. A limiting factor in identifying and therapeutically exploiting this phenotype has been the lack of molecular markers. In the attached manuscript we present evidence for a panel of senescence-specific molecular markers upregulated in both replicative and induced senescence. We also demonstrate that induction of a senescent phenotype in prostate cancer lines using doxorubicin inhibits growth of untreated cancer cells. It is our **hypothesis** that the therapeutic activity induced by chemotherapeutic agents is due, in part, to a senescence-like program of terminal growth arrest. Furthermore, this phenotype inhibits the proliferation of surrounding cells and its presence may predict tumor response to therapy.

Body:

Task 1: **To determine whether senescent tumor cells alter the growth of surrounding prostate cancer cells *in vitro* and *in vivo***.

1. Co-culture and transwell experiments with ratios of senescent and proliferating cells; Generate senescent DU145 and LNCaP using DAC, doxorubicin and Docetaxel; proliferation and cell count; viablity (months 1-9)
2. Boyden chamber assays using ratios of senescent and proliferating DU145 and LNCaP cells (months 3-12)
3. *In vivo* studies using ratios of senescent and GFP-labeled non-senescent DU145 and LNCaP cells (10 animals per tx group; Total 50 for DU145 and 50 for LNCaP); GFP analysis cell count, BrdU proliferation, PI for viability, TUNEL/PARP for apoptosis. Statistical analyses (months 3-12)
4. If an effect on proliferation or invasion is seen then (months 6-24):
5. Repeat transwell and Boyden experiments with neutralizing antibodies to IGF receptors 1 and 2, (if stimulatory response) after western confirmation.
6. Repeat transwell and coculture experiments with neutralizing antibodies to IGFBP3 and 5(if inhibitory response)
7. Selective downregulation of putative effectors in senescent cells using siRNA

Completed. This paper entitled "**Drug-Induced Senescence Bystander Proliferation In Prostate Cancer Cells *In Vitro* and *In Vivo*"** is attached (appendix 1) and has been published. The data and methods (Subtasks 1-6) are included within this manuscript. Additional data (unpublished) indicates that the inhibition of IGF2 prevents the proliferative bystander effect seen with the senescence phenotype (Figure 1). In conjunction with our previous data (Schwarze *et al* JBC, 2002) suggesting IGFBP3 is upregulated during senescence, this highlights the importance of this pathway in senescence induction.

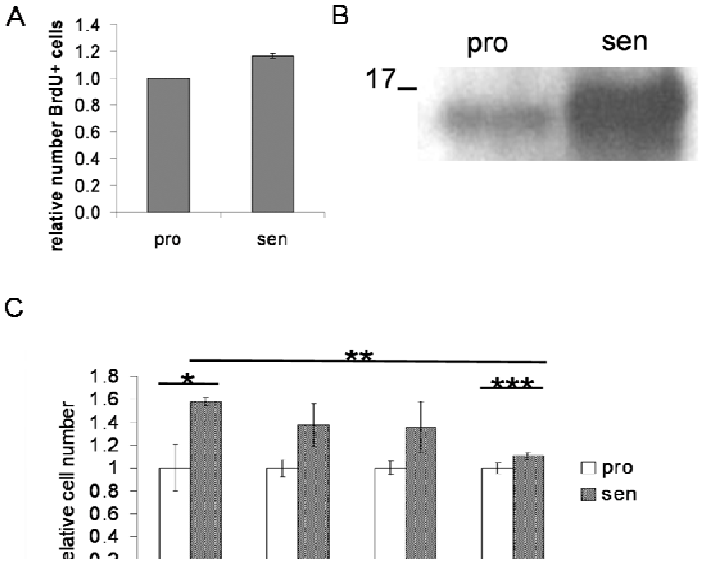

Figure 1: Involvement of secreted proteins in the senescent bystander effect in DU145 cells *in vitro*. (A) BrdU incorporation measured in proliferating DU145-GFP$^{(+)}$ cells co-cultured with proliferating (pro) or senescent (sen) cells in the lower transwell chambers. Three replicates for each experiment (3) were averaged and normalized to the data from cells co-cultured with proliferating cells ($p<0.0001$). (B) IGF2 protein expression in lysates of proliferating and senescent DU145 cells. 20 μg total cell protein in lysates was analyzed by western blotting with anti-IGF2. Specific bands between 10-30kDa (cleavage products) were seen to be increased in senescent cells. (C) Senescence induced proliferation is blocked by anti-IGF2 antibodies. Co-culture experiments were performed as in Figure 1, with anti-IGF2, anti-rabbit secondary or both in minimal media at total concentrations of 40 ng/ml each (1:5,000 dilutions). These results are representative of three independent experiments. Increasing anti-IGF2 or anti-rabbit antibody concentration 3 fold had no effect on proliferation (not shown). (*: $p=0.008$. **: $p<0.0001$. ***:

Senescence is a distinct cellular response induced by DNA damaging agents and other sublethal stressors and may provide novel benefits in cancer therapy. However, in an aging model senescent fibroblasts were found to stimulate the proliferation of co-cultured cells. To address whether senescence induction in cancer cells using chemotherapy induces similar effects, we used GFP-labeled prostate cancer cell lines and monitored their proliferation in the presence of proliferating or doxorubicin-induced senescent cancer cells *in vitro* and *in vivo*. Here we show that the presence of senescent cancer cells increased the proliferation of co-cultured cells *in vitro* through paracrine signaling factors, but this proliferative effect was less than that seen with senescent fibroblasts. *In vivo*, senescent cancer cells failed to increase the establishment, growth or proliferation of LNCaP and DU145 xenografts in nude mice. Senescent cells persisted as long as 5 weeks in tumors. Our results demonstrate that while drug-induced senescent cancer cells stimulate the proliferation of bystander cells *in vitro*, this does not significantly alter the growth of tumors *in vivo*. Coupled with clinical observations, these data suggest that the proliferative effects of senescent cancer cells are negligible and support the further development of senescence induction as therapy. This paper has been supported in another recent publication by Di *et al.* (*Cancer Biol. Ther*, 2008).

Task 2: **To assess for and augment senescence in prostate cancer xenografts and human tumor tissues.**

1. Generate Du145 and LNCaP xenografts in nude mice (months 6-24)

2. Treat with Docetaxel or doxorubicin and harvest at 3 intervals (3 intervals X 10treated/10control per xenograft line = total 60 for DU145 and 60 for LNCaP). GFP analysis cell count, BrdU proliferation, PI for viability, TUNEL/PARP for apoptosis (months 12-30)
3. QPCR and immunohistochemistry for senescence markers (months 12-36)
4. Analysis of human neoadjuvant tissues (10 treated/10 untreated per trial X 2). QPCR and immunohistochemistry for senescence markers (months 24-36)
5. Statistical analyses and correlation with proliferation

Update of Task 2:

Subtasks 1 and 2: We have set up these experiments and completed harvesting these mouse tumors. Nude mice (10+ group) containing DU145 or LNCaP xenografts were treated with Docetaxol(10 mg/kg), Doxorubicin (5mg/kg), or vehicle on Days 0, 2, and 4 (3 experiments). BrdU pellets were implanted on the last treatment day. Animals were sacrificed 5 days after last dose. Tumors harvested for RNA, protein, sectioned for BrDU staining and SA B-gal. Treatment results are displayed in Table 1.

	DU145	**LNCaP**
Docetaxol	TV= -23% BrDU= -17%*	TV= -52% BrDU= -31%
Doxorubicin	TV= -33% BrDU= -35%	TV= -39% BrDU= -33% SA Bgal +

Table 1: Tumor volume (TV) and Proliferation (BrDU) in Prostate Cancer Xenografts Harvested after 4 days.

Subtask 3: Induction of SA-Bgal expression was only found with doxorubicin treatment. We additionally ran RNA for 9 senescence marker genes (Fu et al., Neoplasia, 2007) with the following significant induction results: Du145/Doxorubicin (1/9), LNCaP/Doxorubicin (8/9), Du145/Docetaxol (4/9), LNCaP/Docetaxol (1/9). We conclude that we are able to induce a growth inhibition using these drugs. Using LNCaP a senescence phenotype is found after treatment with doxorubicin. Docetaxol does not induce a robust senescent phenotype. No statistical correlation with proliferation was noted in the xenograft samples when proliferation was correlated with BrDU uptake. Further work with novel agents that induce senescence to a greater extent is detailed in Task 3.

Subtask 4: Given the lack of robust induction of senescent markers utilizing the majority of xenograft models and these drugs, we have had to modify our approach. We have been focusing on developing novel agents that induce a more robust senescence response (see below). Additional markers of senescence focusing on senescent-associated histone acetylation changes (HP1α, HP1γ) and other published markers (IGFBP3, WNT2) are being utilized to determine if any are sensitive enough to reliably detect senescence in treated human tumors of epithelial origin.

Subtask 5: Completed.

Task 3: **To screen for small molecules capable of inducing senescence.**

1. Generate senescence reporter construct using CSPG2 and stably transfect prostate cancer cell lines DU145 and immortalized human prostate epithelial cell line HPV16E7. Select and test reporter. (months 1-6)
2. Optimization of detection conditions (months 6-12)
3. Screen 500 compounds with DU145 to gauge appropriate concentration
4. Screen full 16,000 compound library (months 12-18)
5. Secondary analyses of 25 most active compounds in other prostate cancer cells lines including QPCR for senescence markers, morphology, cell cycle arrest and SA B galactosidase staining. (months 18-30)

Completed. The paper entitled '**High-Throughput Screen to Identify Novel Senescence-Inducing Compounds'** is being revised after submission and is included in Appendix 1. The data and methods (Subtasks 1-5) are included within this manuscript. We had to undertake another approach to developing a screen for senescence-inducing compounds and based this on Hoechst fluorescence and SA-β-gal activity. Our initial approach (Subtask 1) included generating a reporter construct for *Cspg2* containing luciferase and transiently transfected it into the Du145 cell line. Unfortunately, when pooled transfectants were exposed to senescence-inducing doses of doxorubicin (25uM), we were unable to generate a reliable readout for senescence due to low expression levels. The failure of this approach lead to the idea that simply looking at cell number would allow an initial screen and this could be combined with SA-B-gal expression and morphology to screen for senescence induction.

Subtask 2-5: We developed a high-throughput, phenotypic screen to identify compounds in chemical libraries that induce the characteristics of cellular senescence in prostate cancer cells. DU145 was chosen as a model for advanced prostate cancer based on its androgen-independent growth, mutant p53 status, and ability to develop a strong senescent phenotype. The screen is based on the pairing of two compatible staining techniques; one that identifies growth inhibition, and the other SA-β-gal activity (Fig. 1A). The fluorescence of the DNA binding agent Hoechst 33342 was measured to determine cell number after compound exposure for 3 days. In validation studies, the average fluorescence of wells with proliferating cells versus cells induced to senescence with 25nM doxorubicin demonstrated an acceptable Z'-factor of 0.53. This screening-window coefficient indicates a high signal-to-noise and signal-to-background ratio. As this measurement does not differentiate between the induction of senescence or apoptosis, wells with low fluorescence were subsequently visually assessed for SA-*β*-gal staining and senescent morphology.

To identify senescence-inducing compounds, we screened a pilot library of 4160 known bioactive compounds and natural products (KBA) containing structurally diverse characterized compounds, drugs, pollutants and naturally occurring extracts. Using a dose of 10μM in a 96-well format, Hoechst 33342 staining resulted in 625 initial hits (Fig 1B). Compounds with fluorescence >1 standard deviation less than the average of "per plate" data were selected. Wells containing both SA-*β*-gal staining and a senescent morphology (51 compounds) were then assessed for their ability to induce a persistent growth arrest. In triplicate wells, cells were replated and exposed to each of the 51 compounds for 3 days, then allowed to recover following drug removal for an additional 3 days. Cells treated with 9 of the 51 compounds maintained their arrested growth state after removal of the drug (indicated by unchanged Hoechst 33342 intensity; data not shown).

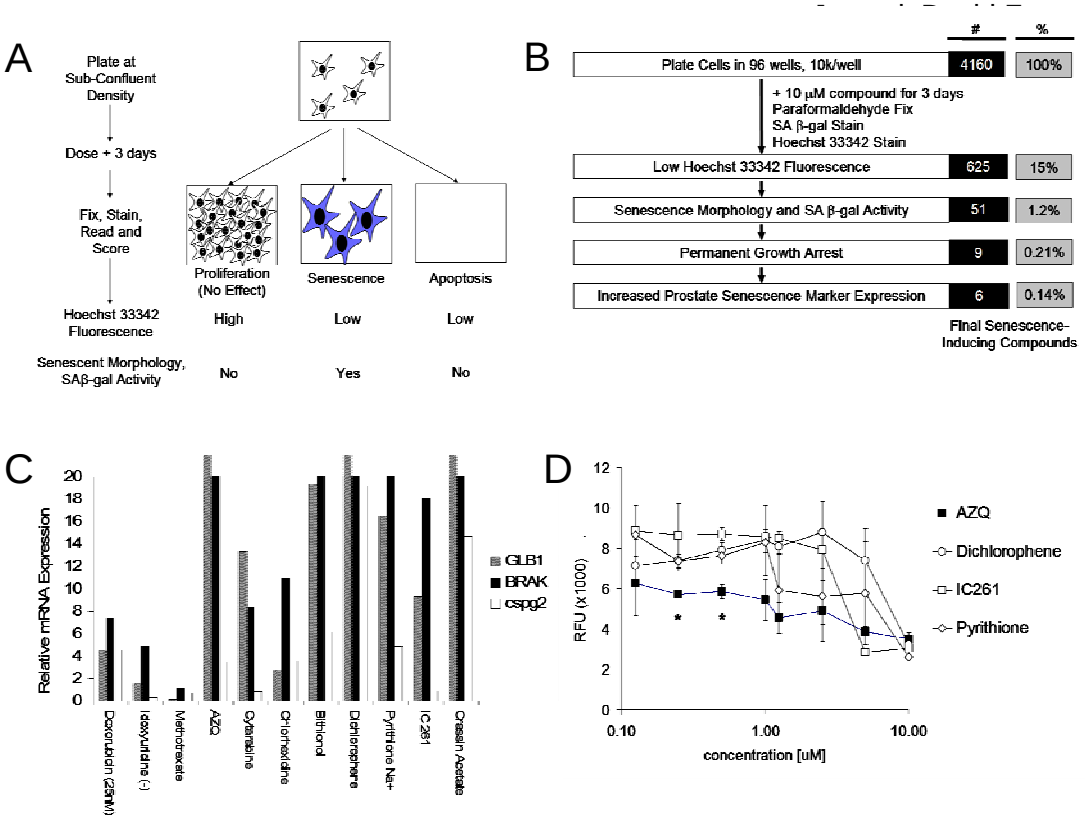

Fig. 1. Screen for senescence-inducing compounds. *A.* Du145 prostate cancer cells were plated on 96 well plates and utilizing robotic high-throughput screens, compounds from a library are plated. After 3 days, proliferation is determined by fluorescence after staining with Hoechst 33342. Low signal wells, indicating either senescence or apoptosis, were then visually examined for the presence of SA-β-gal staining and a senescent (enlarged, flattened) morphology. *B.* Results of the screen on a 4160 compound known bioactive compounds and natural products (KBA) library. Secondary tests included permanent growth arrest, and the induction of other senescent markers. *C.* Expression of senescence marker genes *GLB1, BRAK* and *cspg2* in DU145 cells treated with candidate or control compounds measured by qPCR and normalized to 18S expression. Doxorubicin (25nM) was utilized as a positive control [fu 2006], and one of several quiescence-inducing compounds (idoxyuridine shown) represents a negative control. Data is shown from one experiment performed in duplicate. *D.* AZQ inhibits Du145 cell growth at lower concentrations than other identified compounds. Hoechst 33342 fluorescence was measured after 3 days in wells after treatment with decreasing compound concentrations. Data showing chlorhexidine, bithionol, cytarabine and crassin acetate effectively inhibited proliferation only at doses higher than 1μM are are not shown for sake of clarity. These data represent the results of two independent experiments performed in triplicate. Error bars represent one standard deviation.

These 9 compounds were then tested to determine if they induce the expression of the previously identified senescence marker genes *Glb1, Brak* and *Cspg2*. After a 3 day compound exposure, qPCR was performed on RNA extracted from Du145 prostate cancer cells. Robust induction of all markers was demonstrated with 6 compounds (Fig. 3C) when compared to several quiescence-inducing controls (idoxyuridine shown). This experiment was reproduced using the hormone-dependent LNCaP prostate cancer cell line, confirming robust induction of all senescence marker genes with a final 4 compounds. In sum, this screen has identified compounds (Table 2), out of an original 4160, based on multiple previously established senescence criteria. These compounds are mechanistically diverse, and several had previously been identified as demonstrating growth inhibitory activity in cancer cells.

Table 1: Senescence-inducing agents identified by screening

Compound	PubChem ID	PubChem: Anti-Cancer Activity		Reported Mechanism of Action
		in vitro	*in vivo*	
AZQ	42616	+	-	DNA Alkylating
Bithionol	2406	+	-	N/A
Pyrithione	1570	+	N/A	Zn^{2+} Ionophore
Dichlorophene	3037	+	-	N/A

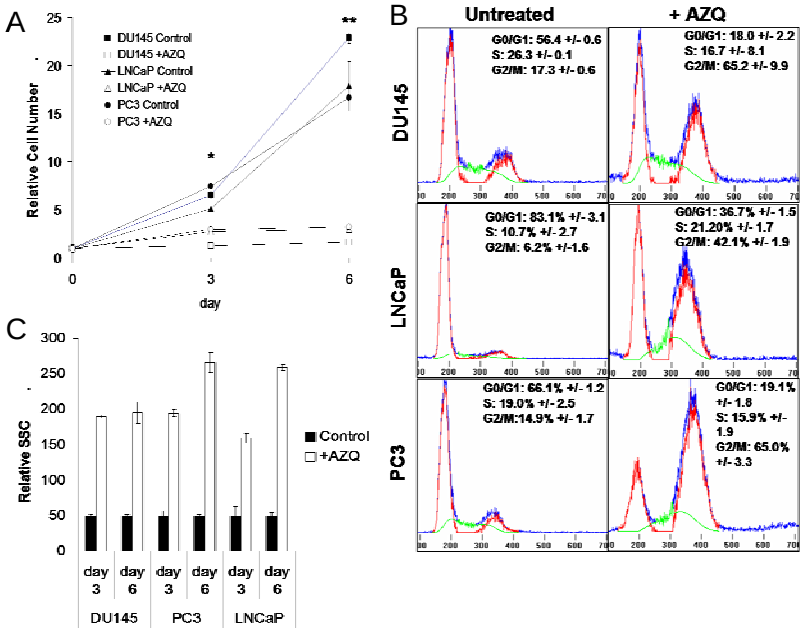

Figure 3: Exposure to senescence-inducing AZQ maintains viability. A. Viability of cells cultured -/+ AZQ, as measured by PI exclusion and cell size (forward scatter), normalized to data from untreated cell samples. (*: p< 0.03). Error bars represent standard error. B. Immunoblot analysis of full length PARP and a-tubulin expression in whole lysates of cells -/+ 250nM AZQ for 72 hr. These results are representative of three independent experiments. C. Detection of SAB-gal activity in whole DU145 cells cultured *in vitro* -/+ AZQ. Original magnification: 400x.

The Compound AZQ Induces A Potent Senescence Growth Arrest *In Vitro* and *In Vivo*. The relative potency of the identified compounds to inhibit cellular proliferation was tested. In 96-well plates, DU145 cells were treated with a range of compound concentrations (0.1-10uM) and the average well fluorescence measured after fixing the cells and staining them with Hoechst 33342 (Fig 1D). AZQ inhibited proliferation to a greater extent at sub-µM concentrations when compared to other identified compounds rendering it the most potent of these agents. Structurally, AZQ is a rationally-designed, lipophillic, DNA-alkylating quinone.

To demonstrate these results were not cell line specific, other prostate cancer cell lines were treated with AZQ and longer-term and complete growth inhibition was shown after drug removal (Figure 2A; p=0.01). Analysis of DNA content in cell lines at the 3 day timepoint shows that AZQ-treated cells accumulate in G2/M and are significantly different than untreated cells (p<0.0001; Fig 2B). The broad distribution of this peak suggests the possibility that this population may include cells arrested at late S phase checkpoints as well. A second characteristic of senescence, increased cellular complexity and size, was measured by flow cytometry using side-scatter(SSC)(10). SSC in viable AZQ-treated cells was increased in all cell lines at both 3 and 6 days (p<0.001; Fig 2C). Viability is another feature of

senescent cells. PI exclusion demonstrates all treated cell lines maintain an average of 71% +/- 4% viable cells after exposure to AZQ at both day 3 and day 6 timepoints when compared to untreated cells ($p < 0.03$; Fig 4A). Western analysis of protein lysates from AZQ treated cells were analyzed to evaluate apoptosis. Both proliferating and senescent cell lines maintain similar amounts of full length PARP without any detectable cleavage products that would be indicative of apoptosis(33) (Fig 4B). Given this and the cell cycle analysis data, the response of these cells to AZQ is largely non-cytotoxic.

Prostate cancer cell lines were then stained for SAB-gal activity, a marker of senescence \ and staining graded from 0 (no staining) to 3 (intense, complete staining). At 3 days after treatment, increased SAB-gal activity was demonstrated in treated cell lines (Fig. 4C).

Finally, we investigated whether AZQ induces a senescent phenotype *in vivo*. Previous studies had demonstrated in other tumor types an *in vivo* cystostatic response (25). As a model system, we generated DU145 xenografts roughly 1cm in size and treated them with a single intraperitoneal injection of 4 mg AZQ/kg body weight or vehicle (Fig 5). No toxicity was noted in the acute setting. Similar to *in vitro* results, increased SAβ-gal activity was observed in DU145 xenograft tumors of mice that were administered AZQ. By contrast, increased SAβ-gal activity was not observed in tumors from control mice injected with PBS vehicle (n=3). Apoptosis induction in these tumors, assessed using antibodies that specifically recognize cleaved PARP(33), showed minimal apoptosis in all tumors independent of AZQ treatment, suggesting that these molecular changes are not associated with

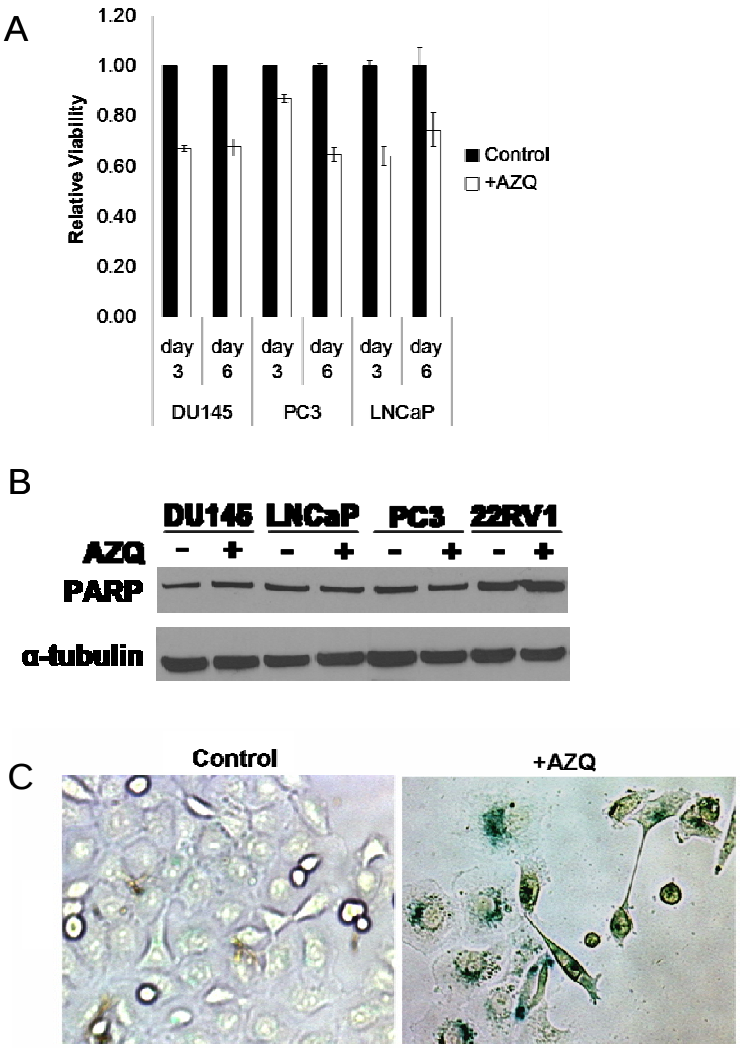

Figure 4. AZQ induces senescence without resulting in apoptosis. Prostate cancer cell lines were cultured in 250 nM AZQ or DMSO(control) for 3 days before drug removal. A. Viability of cells measured by PI exclusion and forward scatter using flow cytometry. Averaged data were normalized to untreated cell samples. A high proportion of cells remained viable in all samples. Error bars represent standard error. B. Immunoblot analysis of full length PARP demonstrates no induction of apoptosis in whole lysates of cells treated with 250nM AZQ for 72 hr. α-tubulin was utilized as a loading control. These results are representative of three independent experiments. C. Bright field microscopy demonstrates increased SA-β-gal activity in DU145 cells cultured with 250nM AZQ for 72 hr (original magnification 400x). SA-β-gal activity was similarly increased in PC3, LNCaP and 22RV1 cells cultured in 250nM AZQ (data not shown). These results are representative of four independent experiments.

apoptosis (data not shown). These results demonstrate the ability of AZQ to be effectively delivered *in vivo* and to induce SAβ-gal activity in DU145 prostate tumor xenografts.

In sum, AZQ to induce a phenotype consistent with senescence growth arrest. These data also validate the ability of our high-throughput screen to identify senescence-inducing compounds.

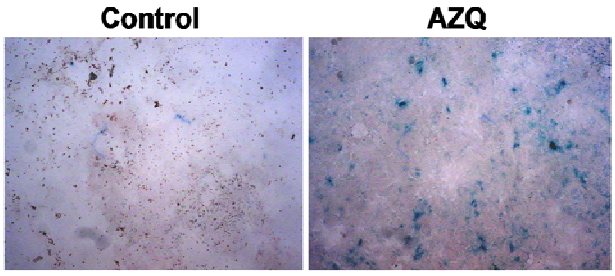

Figure 4: Bright field microscopy of SAB-gal activity in DU145 cells -/+ AZQ *in vitro*. These results are representative of 4 independent experiments.

A manuscript is currently in submission regarding these experiments(appendix). Additional screening of a 16,000 compound library is ongoing. Another paper is being prepared regarding our identification of a novel senescence inducing agent AZQ. We are repeating additional experiments and find it to be and excellent cytostatic drug both *in vivo* and *in vitro*.

Key Research Accomplishments:

- Senescence induces a bystander effect *in vitro,* but not *in vivo.*
- *In vitro* senescence is mediated, in part, by the IGF axis.
- A novel, whole-cell senescence screen has been developed that identifies novel agents that induce senescence robustly.
- Senescence is able to be induced in xenografts in vivo with specific agents.
- AZQ, a quinone, is identified as a novel senescence inducing agent.

Reportable outcomes:

Papers

1. Ewald JA, Desotelle JA, Almassi N and Jarrard DF. Drug-induced senescence bystander proliferating in prostate cancer cells in vitro and in vivo.. *Br J Cancer*, 2008.;98 1244-9.
2. Ewald JA, Peters N, Desotelle JA, Laurila T, Hoffman M, and Jarrard DF. High-Throughput Screen to Identify Novel Senescence-Inducing Compounds. (in revision)
3. Ewald JA, Desotelle JA, Laurila T, Almassi N and Jarrard DF. A Novel Screen Identifies Potent Senescence-Inducing Activity of Diaziquone (AZQ) (in preparation)

Meetings and Abstracts

1. 'A Novel High Throughput Screen Identifies Potent Senescence-Inducing Activity of Diaziquone (AZQ) in Prostate Cancer Cells. Jonathan A. Ewald, Timo Laurila, Nima Almassi, Joshua A. Desotelle, and David F. Jarrard', American Association of Cancer Research Meeting, Washington DC, May 2008.
2. 'A Novel High Throughput Screen Identifies Potent Senescence-Inducing Activity of Diaziquone (AZQ) in Prostate Cancer Cells' Jonathan A. Ewald, Timo Laurila, Nima Almassi, Joshua A. Desotelle, and David F. Jarrard, American Urological Association meeting, Orlando FL, May 2008.
3. 'Androgen ablation generates phenotypic characteristics of senescence' Society for Basic Urologic Research meeting, Pheonix AZ, Nov 2008.
4.

Conclusions:

While drug-induced senescent cells stimulate the proliferation of surrounding cancer cells *in vitro,* this does not significantly affect the longterm growth of bystander cells that might escape senescence induction. These data support further development of senescence-induction strategies for cancer treatment and is a key and novel finding funded by this DOD grant. Additionally, we have developed and validated a novel screen and find that senescence-inducing drugs are infrequently found in the libraries we have screened. These data do suggest that there are compounds that induce drugs specifically. It provides a tool to develop novel senescence-inducing compounds for prostate cancer therapy, as well as providing further insight into mechanisms of senescence induction.

British Journal of Cancer (2008) 98, 1244 – 1249

www.bjcancer.com

Drug-induced senescence bystander proliferation in prostate cancer cells *in vitro* and *in vivo*

JA Ewald[1,2], JA Desotelle[1,3], N Almassi[1] and DF Jarrard*[,1,2,3]

[1]Department of Urology, University of Wisconsin School of Medicine and Public Health, Madison, WI 53792, USA; [2]University of Wisconsin Paul P Carbone Comprehensive Cancer Center, Madison, WI 53792, USA; [3]University of Wisconsin Environmental and Molecular Toxicology Program, 600 Highland Avenue, Madison, WI 53792, USA

Senescence is a distinct cellular response induced by DNA-damaging agents and other sublethal stressors and may provide novel benefits in cancer therapy. However, in an ageing model, senescent fibroblasts were found to stimulate the proliferation of cocultured cells. To address whether senescence induction in cancer cells using chemotherapy induces similar effects, we used GFP-labelled prostate cancer cell lines and monitored their proliferation in the presence of proliferating or doxorubicin-induced senescent cancer cells *in vitro* and *in vivo*. Here, we show that the presence of senescent cancer cells increased the proliferation of cocultured cells *in vitro* through paracrine signalling factors, but this proliferative effect was significantly less than that seen with senescent fibroblasts. *In vivo,* senescent cancer cells failed to increase the establishment, growth or proliferation of LNCaP and DU145 xenografts in nude mice. Senescent cells persisted as long as 5 weeks in tumours. Our results demonstrate that although drug-induced senescent cancer cells stimulate the proliferation of bystander cells *in vitro*, this does not significantly alter the growth of tumours *in vivo*. Coupled with clinical observations, these data suggest that the proliferative bystander effects of senescent cancer cells are negligible and support the further development of senescence induction as therapy.
British Journal of Cancer (2008) **98,** 1244 – 1249. doi:10.1038/sj.bjc.6604288 www.bjcancer.com
Published online 18 March 2008

Keywords: senescence; bystander effect; prostate cancer; proliferation

Senescence is a physiological programme of terminal growth arrest occurring in both normal and immortalised cells in response to telomeric alterations, and also to sublethal stress and inappropriate oncogenic signalling. Senescent cells develop a characteristic phenotype, including an enlarged, flattened morphology, prominent nucleus, senescence-associated heterochromatin foci (SAHF), and senescence-associated β-galactosidase (SAβ-gal) activity (Narita *et al*, 2003; Campisi, 2005; Lee *et al*, 2006). Cancer treatments, including radiation and chemotherapy, induce senescent characteristics in cells. Doxorubicin and cisplatin are more efficient in generating senescence in cell culture than ionising radiation, etoposide or the microtubule-targeting drugs docetaxel and vincristine (Chang *et al*, 1999). Heterogeneous SAβ-gal staining has been observed in sections of frozen human breast tumours after treatment with cyclophosphamide, doxorubicin and 5-fluorouracil (te Poele *et al*, 2002), and in lung tumours, after carboplatin and taxol (Roberson *et al*, 2005). Senescence develops at lower drug concentrations than apoptosis, potentially limiting treatment-related side effects (Schwarze *et al*, 2005).

Senescence may provide a number of unique therapeutic benefits. When senescence is induced by expressing p53 in a murine liver cancer model, an upregulation of inflammatory cytokines triggers an innate immune response that targets the tumour cells (Xue *et al*, 2007). Other studies have suggested senescence may function as an alternative mechanism of tumour inhibition. In mice bearing Eμ-myc lymphomas, treated with cyclophosphamide, when apoptosis was blocked by Bcl-2 overexpression, senescence developed and these animals had improved survival over the apoptotic tumours (Schmitt *et al*, 2002). The recognition that a senescence programme may be reinduced in immortalised and tumorigenic cells by exposure to selected drugs presents a putative target for blocking cancer cell growth.

However, senescence induction may potentially promote tumour growth. Senescent cells express a variety of growth factors and secreted proteins that may stimulate as well as inhibit cell proliferation (Chang *et al*, 2002; Schwarze *et al*, 2002, 2005; Untergasser *et al*, 2002; Bavik *et al*, 2006). In contrast to apoptosis, a programme of cellular destruction, senescent cells persist and remain viable. SAβ-gal activity in cells has been putatively identified in ageing tissues, including skin and benign prostatic hyperplasia specimens (Dimri *et al*, 1995; Choi *et al*, 2000). Consistent with the hypothesis that ageing induces a procarcinogenic environment, fibroblasts passaged to replicative senescence induce the proliferation of local bystander cells both *in vitro* and in xenografts (Krtolica *et al*, 2001; Bavik *et al*, 2006). To determine whether senescent cancer cells generate a bystander effect or not, we chemically induced senescence in prostate cancer cells using doxorubicin and examined their effect on a bystander cancer cells *in vitro* and *in vivo*.

*Correspondence: Dr DF Jarrard; E-mail: jarrard@surgery.wisc.edu
Revised 14 January 2008; accepted 31 January 2008; published online 18 March 2008

MATERIALS AND METHODS

Cell lines and cell culture

DU145 and LNCaP prostate cancer cell lines, and human primary fibroblasts, were cultured and senescence induced by treatment with 25 nM doxorubicin as described previously (Schwarze *et al*, 2005). Polyclonal green fluorescence protein (GFP)$^{(+)}$ cell lines were generated by infecting DU145 and LNCaP cells with pLS-GFP virus and repeated sorting of GFP$^{(+)}$ cells. Resulting cell lines stably express GFP in ~98 and ~80% of DU145- and LNCaP-derived cell lines, respectively. GFP$^{(+)}$ cells in both lines were approximately 100 × brighter than non-labelled cells, as measured by flow cytometry (data not shown).

Cell-counting experiments

For coculture experiments, 50 000 DU145 or 200 000 LNCaP GFP$^{(+)}$ tagged cells and equivalent proliferating or senescent untagged cells or 50 000 senescent primary prostate fibroblasts were plated together in triplicate in 35-mm wells containing growth medium. The following day, cells were washed twice in phosphate-buffered saline (PBS), given minimal medium (50% F12/50% DMEM + penicillin/streptomycin) and returned to 37°C, 5% CO_2. Cells were collected after 2 or 4 additional days in culture. Cell viability in counted samples was determined by annexinV binding (Invitrogen, Carlsbad, CA, USA) and by propidium iodide exclusion. Data were acquired from samples by flow cytometry and analysed using WinMDI v2.8 software (Joseph Trotter, Scripps Research Institute) to calculate the total number of viable GFP$^{(+)}$ cells in each sample.

Counting experiments were repeated using threefold the number of proliferating or senescent cells (from 50 000 to 150 000 cells), or a decreased fraction of senescent cocultured cells (75 and 25% senescent *vs* proliferating), incubated in minimal medium for 4 days and analysed as above.

BrdU incorporation

In cell-counting experiments (above), 20 mM BrdU was added to cell-culture medium, 30 min prior to trypsinisation, and GFP$^{(+)}$ cells were recovered by fluorescence-activated cell sorting. Isolated cells were fixed in 100% ethanol and stored at −20°C. Subsequently, cells were rehydrated and stained for BrdU as described previously (Krtolica *et al*, 2001; Schwarze *et al*, 2003). BrdU incorporation of cells cocultured in transwells did not require cell sorting.

Xenograft cocultures

All animal protocols and studies were conducted in accordance with the guidelines of the Association for Assessment and Accreditation of Laboratory Animal Care International, and approval was obtained from the University of Wisconsin Institutional Animal Care and Use Committee. Male athymic nude mice were obtained from Harlan (Madison, WI, USA). Xenograft tumours were established as described previously (Passaniti *et al*, 1992a, b). DU145-GFP$^{(+)}$ and unlabelled proliferating or senescent DU145 cells (0.5×10^6, each) were injected into the mouse subinguinal fat pad and allowed to develop into xenograft tumours over 5 weeks time. Tumour dimensions were measured at 3, 4 and 5 weeks after injection using a caliper. BrdU was injected into these mice interperitoneally at a concentration of 70 mg kg^{-1} body weight (Christov *et al*, 1993), harvested 2 h later and dissociated into a single-cell suspension from which GFP$^{(+)}$ cells were isolated by fluorescence-activated cell sorting. These were fixed in ice-cold ethanol and stored at −20°C. BrdU incorporation was measured in recovered cells, as mentioned above.

LNCaP xenografts were established by injecting 1×10^6 LNCaP cells alone, with 50% Matrigel (BD Biosciences, San Jose, CA, USA) or with an equal number of senescent LNCaP cells as described (Passaniti *et al*, 1992a, b), and cells were measured as mentioned above. Additionally, xenografts were established using 0.5×10^6 DU145 cells with or without addition of equal number of senescent GFP$^{(+)}$-DU145 cells. Tumours were measured as mentioned above, harvested at 3 and 5 weeks and samples were frozen in OCT for sectioning.

Immunofluorescence staining and microscopy

Ten micrometre sections of xenografts were fixed in PBS + 4% paraformaldehyde/0.2% Triton X-100/10 mM NaF/1 mM $Na3VO_4$ and washed in PBS + 0.2% Triton X-100/10 mM NaF/1 mM $Na3VO_4$ (wash buffer) before incubation in blocking buffer (wash buffer + 10% fetal bovine serum + 1% bovine serum albumin) for 1 h at room temperature. Sections were washed in blocking buffer and incubated with 1 μg ml^{-1} anti-IGF2 as a cellular counterstain (1 : 200 dilution; Santa Cruz Biotechnology, Inc., Santa Cruz, CA, USA; no. sc-5622) overnight at 4°C. Sections were again washed, incubated for 1 h with 200 ng ml^{-1} (1 : 1000 dilution) anti-rabbit-Alexa 594 + 10 ng ml^{-1} Hoechst 33342 (Invitrogen), washed and mounted using ProLong Gold (Invitrogen). Images were captured using an Olympus microscope with mercury lamp, appropriate filters and spot digital camera and imaging software (Diagnostic Instruments Inc., Sterling Heights, MI, USA). Images were merged and visualised using NIH ImageJ (http://rsb.info.nih.gov/ij/).

Statistical methods

Data were analysed, standard deviation and standard error were calculated, and Student's *t*-tests were performed using Microsoft Excel. Error bars in all figures represent one standard deviation in the data.

RESULTS

We generated stable GFP-expressing lines of the hormone-refractory DU145 (p53-inactive) and the androgen-dependent LNCaP (expressing functional p53) prostate cancer cell lines. To monitor the bystander effect of chemically induced senescent cancer cells, GFP$^{(+)}$ cells were cocultured with proliferating or senescent unlabelled cancer cells, collected and analysed by flow cytometry. Both DU145 and LNCaP cells treated with low-dose (25 nM) doxorubicin for 3 days develop a senescent phenotype, increased SAβ-gal staining (Figure 1A), and express previously described senescence marker genes (Schwarze *et al*, 2005).

Initially, DU145-GFP$^{(+)}$ or LNCaP-GFP$^{(+)}$ cells were plated with equal numbers of proliferating or doxorubicin-induced senescent untagged cells and cultured in a minimal serum-free medium for 2 and 4 days. GFP$^{(+)}$ cells cocultured with senescent cells were similar in number to those cocultured with proliferating cells at 2 days (Figure 1B). However, after 4 days, a significant increase in DU145 (1.46 fold; $P < 0.0001$) and LNCaP (1.51 fold; $P = 0.022$) cells was observed when cocultured with senescent cells. Apoptosis of GFP$^{(+)}$ cells, measured by annexin-V binding and propidium iodide exclusion at each time point, was not significantly affected by the presence of senescent cells (<1% in each sample), suggesting that these observed differences were not due to effects on cell survival. Proliferation, measured by BrdU incorporation, was also increased at day 4 (16–21%; $P = 0.003$) in GFP$^{(+)}$ DU145 cells, exposed to senescent cells (Figure 1C). When DU145 and LNCaP cells were cocultured in 0.4 m transwell inserts, preventing contact between the two populations but allowing exposure to common media, BrdU incorporation was similarly increased (20–24%; $P < 0.0001$ and $P < 0.05$, respectively). Given

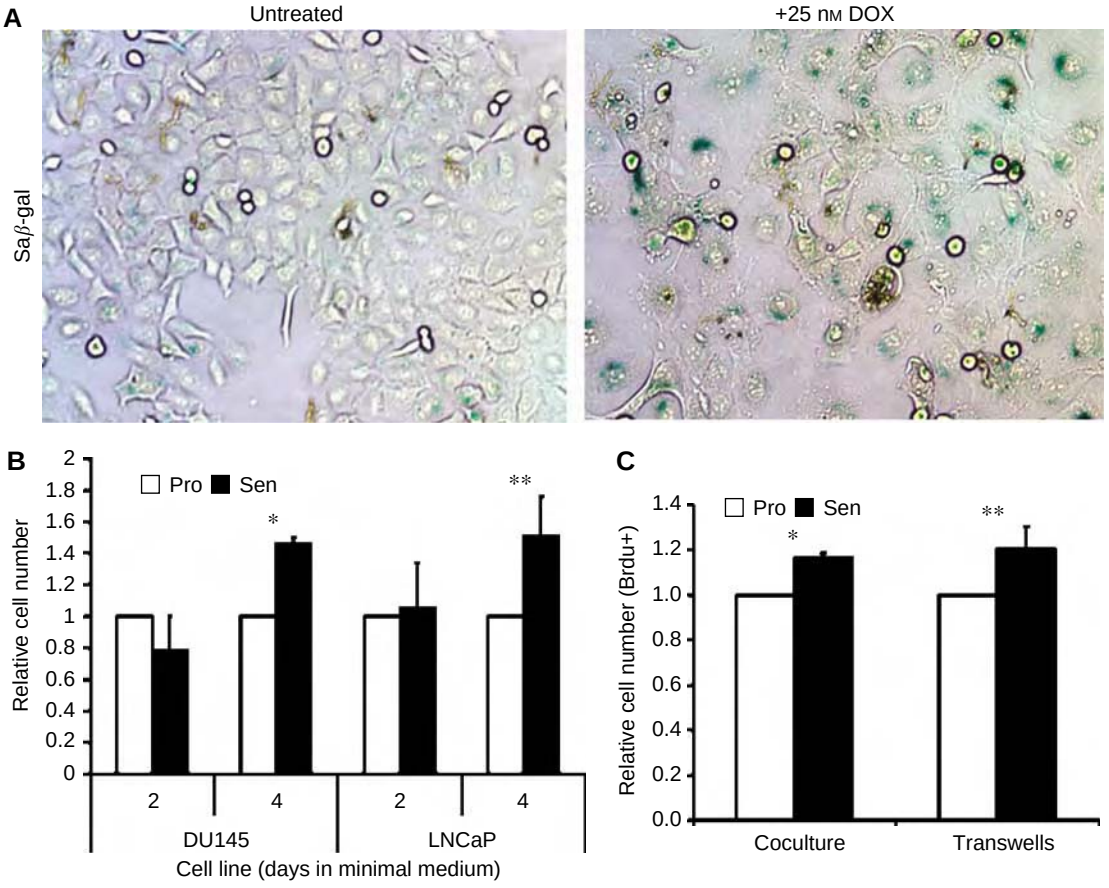

Figure 1 Proliferative bystander effect of drug-induced senescent prostate cancer cells *in vitro*. (**A**) Bright-field images of DU145 cells cultured on cover slips ± 25 nM doxorubicin (DOX) for 3 days, fixed and stained for SA β-gal activity (400 ×). (**B**) Number of proliferating DU145-GFP$^{(+)}$or LNCaP-GFP$^{(+)}$ cells after coculture with proliferating or senescent non-tagged cancer cells measured by flow cytometry. Replicate results were averaged from four independent experiments. These results represent the average fold increase of cell numbers in senescent cocultures relative to proliferative cell data. Error bars represent standard error (*$P<0.0001$; **$P=0.022$). (**C**) BrdU + incorporation in cells after direct coculture (left) and in transwells (right) after 30 min incubation with 20 uM BrdU. The results of three independent experiments were averaged and the numbers of cells from senescent cocultures were normalised to that of proliferating cocultures. Error bars represent standard error (*$P=0.003$, **$P<0.0001$).

the similar magnitude of this proliferative response to the mixing experiments performed on single plates suggested the majority of the growth stimulation observed was induced by secreted soluble factors.

Increasing the numbers of cocultured proliferating and senescent cells threefold in both DU145 and LNCaP cells (150 000 cells) sustained this proliferative response (1.4-fold; in both DU145 and LNCaP cells $P=0.03$ and $P=0.003$, respectively; data not shown) demonstrating that this effect was not an artifact of media depletion. Decreasing the fraction of cocultured senescent cells to 38 and 12% of the total cell population (decrease of 25 and 75% in the unlabelled senescent cells) did not induce proliferation (data not shown). These results demonstrate that a proliferative bystander effect can be stimulated *in vitro* by chemically induced senescent prostate cancer cells through paracrine signalling.

Previously published data have demonstrated a significant proliferative response of bystander cells to senescent fibroblast lines (Krtolica *et al*, 2001; Bavik *et al*, 2006). Therefore, we compared the proliferative bystander response of senescent DU145 cells to three replicatively senescent prostate fibroblast lines generated through prolonged passage in cell culture (Figure 2A). Senescent fibroblasts demonstrated SA-β gal staining and senescent morphology. After 4 days in coculture, the increase in the number of prostate cancer cells exposed to senescent fibroblasts was twice that seen with senescent cancer cells (60 *vs* 30%, respectively; $P<0.01$). We then confirmed the induction (>2 fold) of a number of growth-promoting paracrine factors in our chemically induced senescent DU145 and LNCaP cells (Figure 2B) using qPCR. No increase in expression of these genes (*IGF2, BRAK, FGF11* and *Wnt5a*) was seen in the senescent fibroblast lines. Comparing growth-promoting gene expression data from a number of studies involving fibroblasts, epithelial cells and cancer cells (Schwarze *et al*, 2005; Bavik *et al*, 2006) reveals little overlap when fibroblasts are compared to other cell lines (Figure 2B). In sum, our data show that senescent fibroblasts induce the proliferation of bystander cells *in vitro* significantly more than senescent prostate cancer cells.

Next, we investigated whether senescent cancer cells promote the growth of non-senescent cancer cells in nude mouse tumour xenograft models or not. LNCaP prostate cancer xenografts require additional growth factors, provided by Matrigel™, to establish viable tumours and proliferate (Passaniti *et al*, 1992a, b). To determine if senescence has a similarly permissive effect on xenograft tumour establishment, mice were injected with 1×10^6 LNCaP cells either alone, with 50% Matrigel or with 1×10^6 senescent LNCaP cells ($n=5$ in each group). Six weeks after injection, LNCaP cells coinjected with Matrigel developed into viable tumours in all five animals. In contrast, tumours did not develop under the other conditions (0/10 mice). This demonstrates that chemically induced senescent LNCaP cells do not promote tumour establishment and/or growth of this cell line.

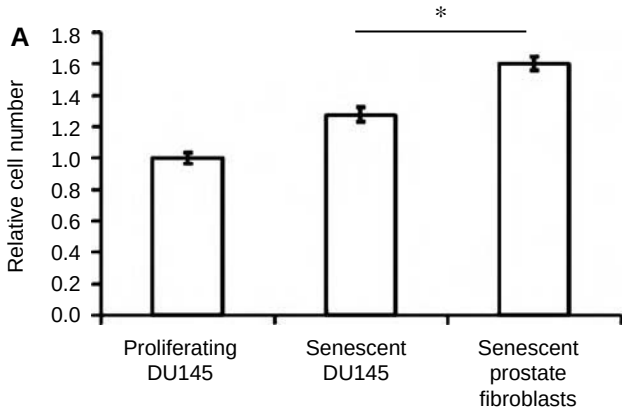

B

Schwarze[1]	Bavik[2]
Senescent prostate cancer cells	Senescent prostate fibroblasts
*Igf2**	*Amphiregulin*
*Fgf11**	*CXCL1*
*Wnt5a**	*CXCL13*
*BRAK**	*CCL20*
MFAP2	*CCL2*
	Cytokine-like Protein C17
	FGF7
	HGF
	IL-8

Figure 2 Bystander proliferation induced to a greater extent by replicatively senescent prostate fibroblasts than senescent prostate cancer cells. (**A**) Number of proliferating DU145-GFP$^{(+)}$ cells cocultured with proliferating or senescent DU145 cells or three independent primary prostate fibroblast cell lines after passage to replicative senescence. Data from all three senescent fibroblast lines were averaged. Results are expressed relative to proliferating coculture data. Error bars represent standard error (*$P<0.01$). Results are representative of two experiments. (**B**) Expression of secreted growth factor genes reported in chemically induced senescent prostate cancer cells and senescent fibroblast ([1]Schwarze *et al*, 2005 *Neoplasia*; [2]Bavik *et al*, 2006. *Canc. Res.* *Increased gene expression confirmed in senescent cancer cells by quantitative RT-PCR in the present study).

Next, we examined the effect of senescent cells on tumour growth in DU145 xenografts using two different approaches. First, we coinjected 0.5×10^6 DU145-GFP$^{(+)}$ proliferating cells with an equal number of unlabelled proliferating or senescent DU145 cells (1×10^6 total) to model the effects of treatment-induced senescence in 50% of tumour cells. Tumours were palpable in both groups after 2 weeks and tumour dimensions were measured 3, 4 and 5 weeks after injection. The average volume of tumours established with or without senescent cells was calculated for each time point. Reflecting the greater number of proliferating cells initially injected, xenografts containing only proliferating cells grew significantly larger than those containing senescent cells after 5 weeks ($P<0.001$) (Figure 3A, left). However, the average exponential rate of tumour growth was not significantly affected by the presence of senescent cells, illustrated by calculating the natural log (ln) of the average tumour volume over time (Figure 3A, right). Control animals, in which only senescent cells were injected, did not develop palpable tumours through the course of these experiments. Mice were injected with 70 mg kg^{-1} body weight BrdU 2 h prior to tumour harvest to measure proliferation in sorted GFP$^{(+)}$ tumour cells (Christov *et al*, 1993). Cells from DU145 tumours established with or without senescent cells and collected after 5 weeks contain similar fractions of proliferating cells as measured by BrdU uptake and DNA profiling (data not shown). As a second approach, we repeated this experiment by beginning with equivalent numbers (0.5×10^6) of proliferating DU145 cells and determining the effect of adding additional (0.5×10^6) senescent cells. Again, the presence of senescent cells did not increase average tumour size or the rate of tumour growth (Figure 3B left, right).

Using senescent GFP$^{(+)}$-DU145 cells in this second approach allowed us to determine whether senescent cells persisted through the growth of these tumours or not. GFP$^{(+)}$ senescent cells were detected in xenograft tumours harvested 3 and 5 weeks after injection. However, at these time points, senescent cells were found infrequently (1–4 cells per section; mean 1 hpf; Figure 3C). SA β-gal analysis of tumour sections demonstrated infrequently stained cells, confirming these findings (data not shown). These results demonstrate that non-proliferating senescent cells become diluted during xenograft growth, yet persist even 5 weeks after injection. Therefore, the presence of chemically senescent cancer cells does not increase the rate of xenograft tumour establishment or growth *in vivo*.

DISCUSSION

Significant interest has been generated regarding the role of senescence as a tumour suppressor and the clinical ramifications of its reactivation in cancer (Schmitt *et al*, 2002; Petti *et al*, 2006; Xue *et al*, 2007). Potential exists for development of therapeutic compounds that specifically induce senescence in cancer cells (Roninson, 2003). However, concerns have been raised regarding the promoting effect of senescent cancer cells on the tumour microenvironment, similar to that seen with senescent fibroblasts (Kahlem *et al*, 2004). Our results demonstrate that a limited proliferative response occurs *in vitro* with chemically induced senescent cells when compared to senescent fibroblasts (Figure 2A). However, this bystander effect does not affect xenograft tumour establishment or the growth of non-senescent bystander tumour cells *in vivo* (Figure 3).

Using multiple cell types and combinations, senescent cells did not impact *in vivo* tumour growth or proliferation. When xenografts were established using proliferating cells with and without senescent cells, tumours were consistently smaller in the presence of senescent cells (Figure 3B). We acknowledge that a transient increase in proliferation may be induced prior to the development of a palpable tumour, but clearly, the long-term impact on tumour size was not significant. Technically similar mixing experiments in immune-deficient mice have been performed using senescent fibroblasts and a stimulatory effect was easily demonstrated using multiple immortalised and tumorigenic cell lines (Krtolica *et al*, 2001; Parrinello *et al*, 2005; Bavik *et al*, 2006). *In vivo,* these studies utilised equivalent numbers of proliferating and senescent cells similar to our methods. Our data clearly show the lack of a stimulatory response when senescent cancer cells are mixed with proliferating cancer cells in tumours. Furthermore, with current chemotherapy regimens, senescent cells appear at a much lower frequency (<20%) than those tested in our experiments (te Poele *et al*, 2002; Roberson *et al*, 2005).

As part of our study, we contrasted, *in vitro*, the bystander effect of senescent fibroblasts to that seen with chemically induced senescent cancer cells. Using our quantitative and reproducible model, the *in vitro* proliferative effect of senescent cancer cells was noted to be 40–50% of that seen with senescent fibroblasts. Our

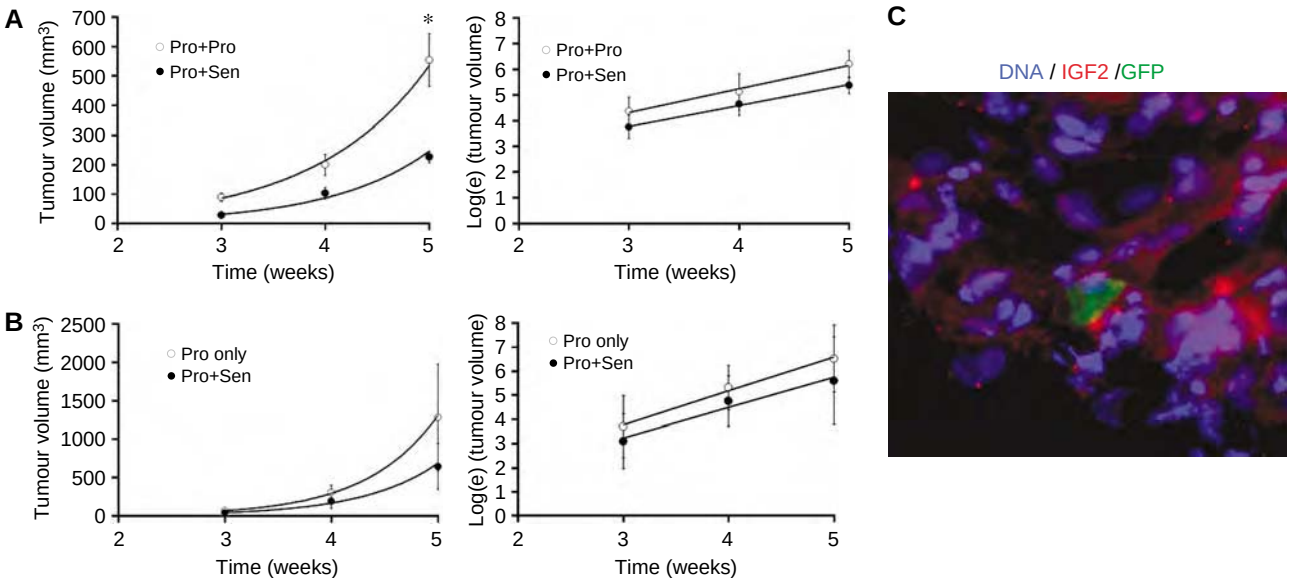

Figure 3 Xenograft tumour growth is not promoted by senescent DU145 cells. (**A**) Average size (left) and natural log of tumour size (right) of prostate xenograft tumours established using DU145-GFP$^{(+)}$ cells (0.5×10^6) mixed with an equal number proliferating (Pro + Pro) or senescent (Pro + Sen) cells and measured for 5 weeks. Error bars represent standard error (*$P<0.001$). Fit equations: (left) (Pro + Pro): $y = 5.491e^{0.913x}$ ($R^2 = 0.996$); (Pro + Sen): $y = 1.362e^{1.039x}$ ($R^2 = 0.981$); (right) (Pro + Pro): $y = 0.917x + 1.565$ ($R^2 = 0.989$); (Pro + Sen): $y = 0.813x + 1.340$ ($R^2 = 0.997$). (**B**) Average size (left) and natural log of tumour size (right) of prostate xenograft tumours established using DU145 (0.5×10^6) cells alone (Pro only) or with an equal number of additional senescent GFP$^{(+)}$-DU145 cells (Pro + Sen). Error bars represent standard error. Fit equations: (left)(Pro only): $y = 0.739e^{1.491x}$ ($R^2 = 0.999$); (Pro + Sen): $y = 0.576e^{1.417x}$ ($R^2 = 0.994$); (right)(Pro only): $y = 1.41x - 0.458$ ($R^2 = 0.994$); (Pro + Sen): $y = 1.254x - 0.527$ ($R^2 = 0.966$). (**C**) Xenograft tumour section containing a senescent GFP$^{(+)}$-DU145 cell. Hoechst 33342 (blue) was used to stain nuclei and anti-IGF2 (red) was used to stain cytoplasm (400 ×). This image is representative of sections from 10 xenograft tumours containing 1–4 GFP$^{(+)}$ cells per section (mean: 1 hpf).

quantitative PCR analysis confirmed the results of studies that show significant variation between growth-promoting genes expressed by senescent epithelial cells, fibroblasts and cancer cells (Chang *et al*, 2002; Schwarze *et al*, 2002, 2005; Untergasser *et al*, 2002; Zhang *et al*, 2003; Bavik *et al*, 2006). The finding that gene expression perturbations during senescence differ greatly between fibroblasts and epithelial cells, but show physical clustering on DNA, has been thought to reflect the altered chromatin structure seen during senescence (Zhang *et al*, 2003). These changes are likely to be even more marked in cancer cells containing deletions, duplications and distorted nuclear structure.

In vivo, the expression of secreted extracellular matrix, growth factors and surface receptor proteins differs markedly from cells cultured *in vitro* (Gieseg *et al*, 2004). This disparity in the tumour microenvironment may contribute to the lack of induction of proliferation in response to senescent cells *in vivo*. As an example, IGF2 protein expression is clearly elevated in senescent cancer cells *in vitro,* but the expression of IGF2 protein does not quantitatively differ *in vivo*, when senescent and proliferating cells are compared (data not shown). A unique aspect of our study is the demonstration of a persistence of senescent cells in tumours as long as 5 weeks after injection. They represent a small population at this time point, less than 1%, due to expansion of the proliferating population, which doubles in roughly 48 h (Passaniti *et al*, 1992a, b). Senescent cells have been noted in the skin of elderly individuals (Dimri *et al*, 1995) and in melanocytic naevi (Michaloglou *et al*, 2005). Our data in a xenograft model would support the persistence of these cells in various organs.

Placing senescence induction in the context of cancer treatment, our results suggest that the specific induction of senescence in prostate tumour cells would not promote tumour growth. Accumulating data suggest that senescent cells may occur *in vivo* after the treatment of tumours with chemotherapy, in approximately 40% of breast tumours after treatment using a CAF regimen (te Poele *et al*, 2002). Other observations support that senescence *in vivo* is a beneficial phenotype by inducing a cellular immune response (Petti *et al*, 2006; Xue *et al*, 2007) and demonstrating a survival advantage when compared to solely apoptotic responses (Schmitt *et al*, 2002). Recently, senescent cells were identified in human melanocytic nevi, a benign, stable skin lesion, supporting its function as a long-term tumour-suppressive mechanism (Michaloglou *et al*, 2005). In this case, there are no apparent signs of enhanced bystander proliferation or increased local carcinogenesis. Staining for senescent cells has also been identified in benign prostatic hyperplasia tissues, a common benign entity not associated with cancer (Choi *et al*, 2000). In conclusion, our data demonstrate that the presence of chemically senescent prostate cancer cells does not significantly enhance the growth of tumour xenografts, providing further rationale for the development of anticancer strategies that efficiently induce senescence in advanced cancers.

ACKNOWLEDGEMENTS

We acknowledge the helpful flow cytometry expertise of Kathy Schell, Colleen Urben and Joel Puchalski; Dr Glenn Leverson and Dr Alejandro Munoz of the Department of Surgery (University of Wisconsin Hospital) for help with statistical analysis and data interpretation.

This work was supported by the National Institutes of Health (R01CA97131) and the University of Wisconsin, George M O'Brien Urology Research Center (1P50DK065303) and the John Livesey endowment. JE is supported through the NIH training Grant T32 CA009681 to the University of Wisconsin McArdle Laboratory Cancer Biology Training Program. No financial relationship between any of the authors and the subject matter.

REFERENCES

Bavik C, Coleman I, Dean JP, Knudsen B, Plymate S, Nelson PS (2006) The gene expression program of prostate fibroblast senescence modulates neoplastic epithelial cell proliferation through paracrine mechanisms. *Cancer Res* **66:** 794 – 802

Campisi J (2005) Senescent cells, tumor suppression, and organismal aging: good citizens, bad neighbors. *Cell* **120:** 513 – 522

Chang BD, Broude EV, Dokmanovic M, Zhu H, Ruth A, Xuan Y, Kandel ES, Lausch E, Christov K, Roninson IB (1999) A senescence-like phenotype distinguishes tumor cells that undergo terminal proliferation arrest after exposure to anticancer agents. *Cancer Res* **59:** 3761 – 3767

Chang BD, Swift ME, Shen M, Fang J, Broude EV, Roninson IB (2002) Molecular determinants of terminal growth arrest induced in tumor cells by a chemotherapeutic agent. *Proc Natl Acad Sci USA* **99:** 389 – 394

Choi J, Shendrik I, Peacocke M, Peehl D, Buttyan R, Ikeguchi EF, Katz AE, Benson MC (2000) Expression of senescence-associated beta-galactosidase in enlarged prostates from men with benign prostatic hyperplasia. *Urology* **56:** 160 – 166

Christov K, Swanson SM, Guzman RC, Thordarson G, Jin E, Talamantes F, Nandi S (1993) Kinetics of mammary epithelial cell proliferation in pituitary isografted BALB/c mice. *Carcinogenesis* **14:** 2019 – 2025

Dimri GP, Lee X, Basile G, Acosta M, Scott G, Roskelley C, Medrano EE, Linskens M, Rubelj I, Pereira-Smith O, Peacocke M, Campisi J (1995) A biomarker that identifies senescent human cells in culture and in aging skin *in vivo*. *Proc Natl Acad Sci USA* **92:** 9363 – 9367

Gieseg MA, Man MZ, Gorski NA, Madore SJ, Kaldjian EP, Leopold WR (2004) The influence of tumor size and environment on gene expression in commonly used human tumor lines. *BMC Cancer* **4:** 35

Kahlem P, Dorken B, Schmitt CA (2004) Cellular senescence in cancer treatment: friend or foe? *J Clin Invest* **113:** 169 – 174

Krtolica A, Parrinello S, Lockett S, Desprez PY, Campisi J (2001) Senescent fibroblasts promote epithelial cell growth and tumorigenesis: a link between cancer and aging. *Proc Natl Acad Sci USA* **98:** 12072 – 12077

Lee BY, Han JA, Im JS, Morrone A, Johung K, Goodwin EC, Kleijer WJ, DiMaio D, Hwang ES (2006) Senescence-associated beta-galactosidase is lysosomal beta-galactosidase. *Aging Cell* **5:** 187 – 195

Michaloglou C, Vredeveld LC, Soengas MS, Denoyelle C, Kuilman T, van der Horst CM, Majoor DM, Shay JW, Mooi WJ, Peeper DS (2005) BRAFE600-associated senescence-like cell cycle arrest of human naevi. *Nature* **436:** 720 – 724

Narita M, Nunez S, Heard E, Narita M, Lin AW, Hearn SA, Spector DL, Hannon GJ, Lowe SW (2003) Rb-mediated heterochromatin formation and silencing of E2F target genes during cellular senescence. *Cell* **113:** 703 – 716

Parrinello S, Coppe JP, Krtolica A, Campisi J (2005) Stromal-epithelial interactions in aging and cancer: senescent fibroblasts alter epithelial cell differentiation. *J Cell Sci* **118:** 485 – 496

Passaniti A, Adler SH, Martin GR (1992a) New models to define factors determining the growth and spread of human prostate cancer. *Exp Gerontol* **27:** 559 – 566

Passaniti A, Isaacs JT, Haney JA, Adler SW, Cujdik TJ, Long PV, Kleinman HK (1992b) Stimulation of human prostatic carcinoma tumor growth in athymic mice and control of migration in culture by extracellular matrix. *Int J Cancer* **51:** 318 – 324

Petti C, Molla A, Vegetti C, Ferrone S, Anichini A, Sensi M (2006) Coexpression of NRASQ61R and BRAFV600E in human melanoma cells activates senescence and increases susceptibility to cell-mediated cytotoxicity. *Cancer Res* **66:** 6503 – 6511

Roberson RS, Kussick SJ, Vallieres E, Chen SY, Wu DY (2005) Escape from therapy-induced accelerated cellular senescence in p53-null lung cancer cells and in human lung cancers. *Cancer Res* **65:** 2795 – 2803

Roninson IB (2003) Tumor cell senescence in cancer treatment. *Cancer Res* **63:** 2705 – 2715

Schmitt CA, Fridman JS, Yang M, Lee S, Baranov E, Hoffman RM, Lowe SW (2002) A senescence program controlled by p53 and p16INK4a contributes to the outcome of cancer therapy. *Cell* **109:** 335 – 346

Schwarze SR, DePrimo SE, Grabert LM, Fu VX, Brooks JD, Jarrard DF (2002) Novel pathways associated with bypassing cellular senescence in human prostate epithelial cells. *J Biol Chem* **277:** 14877 – 14883

Schwarze SR, Fu VX, Desotelle JA, Kenowski ML, Jarrard DF (2005) The identification of senescence-specific genes during the induction of senescence in prostate cancer cells. *Neoplasia* **7:** 816 – 823

te Poele RH, Okorokov AL, Jardine L, Cummings J, Joel SP (2002) DNA damage is able to induce senescence in tumor cells *in vitro* and *in vivo*. *Cancer Res* **62:** 1876 – 1883

Untergasser G, Koch HB, Menssen A, Hermeking H (2002) Characterization of epithelial senescence by serial analysis of gene expression: identification of genes potentially involved in prostate cancer. *Cancer Res* **62:** 6255 – 6262

Xue W, Zender L, Miething C, Dickins RA, Hernando E, Krizhanovsky V, Cordon-Cardo C, Lowe SW (2007) Senescence and tumour clearance is triggered by p53 restoration in murine liver carcinomas. *Nature* **445:** 656 – 660

Zhang H, Pan KH, Cohen SN (2003) Senescence-specific gene expression fingerprints reveal cell-type-dependent physical clustering of up-regulated chromosomal loci. *Proc Natl Acad Sci USA* **100:** 3251 – 3256

High-Throughput Screen to Identify Novel Senescence-Inducing Compounds

Jonathan A. Ewald PhD[1, 2], Noel Peters MS[2], Joshua A. Desotelle[3], F. Michael Hoffmann PhD[2, 4] and David F. Jarrard MD[1,2,3, †]

[1]Department of Urology; [2]Paul P. Carbone Comprehensive Cancer Center; [3]Department of Environmental Toxicology; [4]McArdle Laboratory for Cancer Research. University of Wisconsin – Madison. Madison, WI. 53792

Running Title: Screen for Senescence Inducing Drugs

Keywords: cellular senescence; high-throughput screen; prostate; prostate cancer

Financial Support: This work was supported by the National Institutes of Health(R01CA97131), the University of Wisconsin George M. O'Brien Urology Research Center(1P50DK065303), the John Livesey endowment and the Department of Defense Prostate Cancer Research Program(DAMD17-02-1-0163). J.A.E. is supported through an NIH Ruth L. Kirchstein National Research Service Award(T32 CA009681-14).

[†]Corresponding author: 600 Highland Avenue, K6/530, Madison, WI 53792, USA; Telephone: 608-263-9534; Fax: 608-265-8133; E-mail: jarrard@surgery.wisc.edu.

Abstract

Cellular senescence is a persistently growth-arrested phenotype in normal and transformed cells induced by non-cytotoxic stress. Research into the induction of cellular senescence as cancer therapy has been hindered by a lack of compounds that efficiently induce this response. We describe a semi-automated high-throughput phenotypic assay to identify compounds that induce senescence using prostate cancer cells cultured in 96 well plates. Primary hits are identified by the induction of growth arrest after 3 days measured by Hoechst 33342 fluorescence. A secondary visual assessment of senescence-associated ß-galactosidase staining and morphology in the same wells distinguishes senescence from quiescence, apoptosis and other false-positives. This method was used to screen a 4160 compound library of known bioactive compounds and natural products. Candidate compounds were further selected based on persistent growth arrest after drug removal and increased expression of previously described senescence marker genes *Glb1*, *Cspg2* and *BRAK*, identifying 4 diverse compounds not previously associated with senescence. We further show cells exposed to these compounds maintain viability, with few cells exhibiting propidium iodide/annexin V staining or caspase 3 cleavage, each molecular characteristics of apoptosis. This is the first successful assay to identify novel agents from compound libraries that induce senescence in cancer cells.

Introduction

There is increasing interest in the development of oncostatic compounds that prevent the growth and progression of cancers without cytotoxicity. Evidence suggests that such agents may increase patient survival while minimizing treatment side-effects and chemoresistance in prostate and other cancers(1). The induction of accelerated cellular senescence is one mechanism by which this effect may be achieved(2, 3). Cellular senescence is a general program of persistent growth arrest in response to sub-lethal stresses in both normal non-transformed and immortalized transformed cells(4). Senescent cells cease dividing, become insensitive to mitogenic and certain apoptotic stimuli, and develop a phenotype similar to replicatively exhausted cells, exhibiting a characteristic enlarged and flattened morphology and increased senescence-associated ß-galactosidase (SA-β-gal) staining activity (Fig 1)(3, 5, 6). While ongoing studies seek to identify ubiquitous markers and regulators of senescence, SA-β-gal staining remains a standard and accepted marker used to identify senescent cells(5, 6).

Agents that generate oxidative stress, DNA damage and/or stress-related signaling induce cellular senescence(7). These include both endogenous processes including telomere loss, accumulated oxidative damage, dysregulated oncogene activity, and exogenous factors such as chemicals, viral oncogenes, UV light, and ionic radiation. In aging organisms, cellular senescence represents an *in vivo* tumor suppressor mechanism that limits the proliferation of damaged cells(5). This frequently involves the activity of tumor suppressors p53 and pRb,

and increased protein expression of cyclin-dependent kinase (CDK) inhibitors $p21^{waf1/cip1}$, $p16^{ink4a}$ and $p27^{kip1}$ (5). Cells exhibiting SA-β-gal staining and other senescence characteristics have been observed in benign lesions including lung adenomas(8), melanocytic naevi(9, 10), and prostatic intraepithelial neoplasia(11). A similar senescent state can be chemically induced in prostate and other cancer cell lines *in vitro,* independent of p53, Rb and other tumor suppressor pathways (12-15). In humans, SA-β-gal staining has been observed in lung tumors (14) and breast tumors after treatment with genotoxic drugs (16). Evidence in some studies suggest that the induction of senescence may provide benefits as a cancer treatment, including increased patient survival and stimulation of immune responses(2, 17-19). However, the investigation of drug-induced senescence has been hampered by the lack of identified compounds that effectively induce this response.

Toward this end, we have developed a rapid and reliable semi-automated duplexed high-throughput assay to screen libraries for novel compounds that induce senescence in prostate cancer cells. Cells are stained concurrently with DNA-binding Hoechst 33342 and for SA-β-gal activity, and compounds are selected on the basis of both growth inhibition associated with senescence and the phenotypic changes that result from its induction. Candidate compounds can then be further validated for induction of persistent growth arrest and expression of senescence marker genes. Using this assay, we screened a library of 4160 known bioactive compounds and natural products, identifying 4 compounds not previously associated with senescence induction.

Materials and Methods

Compound Library. Compounds used in this study were stored, maintained and handled by the Keck-University of Wisconsin Carbone Comprehensive Cancer Center (Keck-UWCCC) Small Molecule Screening Facility (hts.wisc.edu/Index.htm). The compound library used for screening consists of 3 commercially available collections totaling 4,160 compounds. This includes: 2000 diverse FDA approved drugs and natural products (Microscource Discovery Systems, Inc; Gaylordsville, CT); the 1280 compound LOPAC^{1280} library of diverse characterized compounds (Sigma; St Louis, MO); and 880 characterized compounds (Prestwick Chemicals; Illkirch, FR). Compounds were dissolved in DMSO and stored in 384 well plates at -80°C. Included on each 384 well plate are 64 DMSO negative controls. Further details can be obtained at http://hts.wisc.edu/Libraries.htm#kba.

AZQ (NSC 182986) was provided by the Developmental Therapeutics Program, Division of Cancer Treatment and Diagnosis, National Cancer Institute, National Institutes of Health. Bithionol, Dichlorophene, Na^+ pyrithione and Camptothecin were purchased from Sigma and stock compounds were dissolved in DMSO and stored at -80°C. Compound structures were obtained from PubChem (http://pubchem.ncbi.nlm.nih.gov/).

Multiplexed Cell Growth-Inhibition/SA-β-gal Assay Biomek FX robotic high-throughput fluid handling instruments (Beckman-Coulter; Fullerton, CA) were

operated by the Keck-UWCCC Small Molecule Screening Facility (hts.wisc.edu/Index.htm). DU145 cells were cultured as previously described(15), suspended at a density of $1x10^4$ cells/100μl culture medium and 100μl/well added to 96 well plates(Corning #3906). Library compounds were administered to cells at a final concentration of 10μM and incubated for 3 days. Cells were then washed in warm PBS, fixed and stained for SA-β-gal activity overnight, as previously described(6) using 100μl/well. Cells were again washed in PBS and incubated at room temperature in PBS + 10μg/ml Hoechst 33342(Invitrogen; Carlsbad, CA) for 10 min. Hoechst 33342 fluorescence (ex/em: 355nm/460nm) was measured using a Victor V-3 high-throughput stacking plate reader (Perkin-Elmer; Waltham, MA). In control experiments, cells were cultured in medium containing 25nM Doxorubicin (Sigma) to induce senescence (15), and Hoechst 33342 fluorescence was measured to calculate Z' compared to proliferating cells, as previously described(20).

In the pilot screen, wells in which fluorescence was more than 1 standard deviation (SD) below the average of 384 data points (one drug plate) were then visually inspected by three independent observers to assess the intensity of SA-β-gal staining (0-4) and the presence or absence of senescence morphology. Selected compounds were subsequently assessed for induction of persistent growth arrest by culturing cells in duplicate wells of 96 well plates with 3 days drug exposure followed by removal of drug and 3 additional days of incubation with fixing and staining as above. Hoechst 33342 fluorescence of these cells were compared to that of cells exposed to 25nM Doxorubicin (n=24) as a positive

control. Wells with Hoechst fluorescence less than the average of those treated with 25nM Doxorubicin were visually inspected to confirm growth inhibition and development of senescence-like morphology.

Prostate Senescence Marker Gene Expression DU145 or LNCaP cells were cultured as previously described(15). These cells were split to duplicate wells in 96 well plates at density of $1x10^4$ cells/100μl culture medium and 100μl/well and incubated overnight. Cells were then treated with 10μM concentration of each selected compound, and incubated for 3 days. RNA was isolated from cells, reverse transcribed, and *Glb1, BRAK, Cspg2,* and *18S* gene expression were measured by quantitative real-time PCR (qPCR) using an iCycler thermocyler and MyiQ software (BioRad; Hercules, CA) as previously described(15). Expression of genes in each sample was standardized to 18S measurements, and relative expression of treated samples was normalized to that of untreated cells.

Cell Viability and Apoptosis DU145 prostate cancer cells were cultured as previously described(15). To monitor cell viability, 50,000 of each cell line were seeded in 6-well plates in triplicate per experimental condition. After overnight incubation, DMSO vehicle, 250nM AZQ, 10μM Bithionol, 10μM Dichlorophene or 2.5μM Na^+ pyrithione were added to cells, incubated for three days, trypsinized and cellular viability was assessed by propidium iodide exclusion(21) and Alexa 488-conjugated Annexin V staining (A13201: Invitrogen) according to

manufactured instructions. The fractions of non-staining viable cells and apoptotic cells stained with propidium iodide and/or Annexin V in each sample were measured by flow cytometry. As a positive apoptotic control, triplicate wells of DU145 cells were exposed to 10μM Camptothecin for 6 hours prior to harvest, staining and analysis.

Additionally, compounds were assessed for their ability to induce cleavage of caspase 3, an indicator of apoptosis. Approximately $1x10^6$ DU145 cells were cultured in 100mm plates and similarly left untreated or exposed to selected compounds for 3 days, as above. As a positive control for apoptosis induction, cells were also exposed to 10μM Camptothecin for 6 hours prior to lysis. Lysates were generated and analyzed by immunoblotting as previously described(22) using antibodies recognizing full length (#9662) and cleaved caspase 3 (#9961: Cell Signaling Technology, Danvers, MA), and α–tubulin (CP06: Calbiochem, San Diego, CA).

Results

Method Development. The aim of this study was to develop a high-throughput screen to identify compounds in chemical libraries that induce characteristics of cellular senescence in prostate cancer cells. DU145 cells were selected as a model of advanced prostate cancer based on their androgen-independent growth, mutant p53 and Rb status(23), and the ability to develop phenotypic senescence in response to chemical treatment (15). This method is based on the pairing of two compatible staining techniques that allow detection of growth

inhibition and assessment of SA-β-gal activity in the same well. Cells are plated into 96 well plates, drugs are added, and after 3 days incubation they are fixed and stained for SA-β-gal overnight followed immediately by staining with the fluorescent DNA-binding Hoechst 33342 (Fig 2). Hoechst 33342 fluorescence can be measured in each well using a high-throughput plate reader to quickly identify wells with decreased fluorescence, indicative of growth inhibition. These infrequent wells can then be assessed visually to determine the extent of SA-β-gal staining, further selecting compounds for additional investigation.

Control experiments were performed to validate the ability of Hoechst 33342 fluorescence to discriminate proliferating cells from senescent and apoptotic cells using increasing doses of Doxorubicin. Exposure of DU145 cells to 25nM Doxorubicin had been previously shown to induce a senescent morphology and SA-β-gal expression (15). Our repeated experiments demonstrate that doses of Doxorubicin 25nM and higher reduce fluorescence significantly ($p<0.003$) when compared to untreated or 5nM Doxorubicin after 3 days exposure (Fig 3A). We then compared the fluorescence of untreated proliferating cells to cells induced to senescence with 25nM Doxorubicin (Fig 3B) and repeated experiments generated an average Z'-factor of 0.53(20). This calculated coefficient indicates a suitably high signal-to-noise ratio to identify senescence-like growth inhibition in a high-throughput format (Fig 3B). Increased concentrations of Doxorubicin (100nM and 250nM) induced apoptosis and cytotoxicity with fluorescence similar to blank wells. We further found that although the fluorescence of senescent cells is statistically different from that of

cytotoxic doses ($p<0.05$), the Z'-factor of these experiments was less than 0.5 indicating the need for additional analyses to distinguish senescence from cell death.

Therefore, we incorporated the widely utilized marker SA-β-gal to identify senescent cells(6). SA-β-gal staining did not interfere with Hoechst 33342 fluorescence readings when cells were co-stained (data not shown). Experiments performed to determine whether SA-β-gal could be detected utilizing a plate reader (OD_{600}) failed to generate the desired sensitivity. Consequently, we had observers visually score, using a phase-contrast microscope, both SA-β-gal staining (0-4) and senescent morphology in those wells found to have fluorescence greater than one standard deviation less than the average plate data. Wells found to contain robust staining (3 or 4) and senescent morphology (Fig 1) were selected for further investigation.

Pilot Screen. We used this method to screen a library of 4160 known structurally diverse characterized bioactive compounds and natural products for senescence-inducing activity. After incubating cells with 10μM of each compound or DMSO for 3 days, cells were fixed, stained and Hoechst fluorescence measured. Wells with fluorescence >1 standard deviation less than the plate averages resulted in 625 initial hits from the library (Fig 4). Subsequent visual scoring of these wells for robust SA-β-gal expression and senescence morphology identified 226 compounds as cytotoxic and 51 compounds as inducing a senescent phenotype(1.2% of the library).

Confirmatory Assays. We tested whether these compounds induce a proliferation arrest in cells that persists after drug removal consistent with senescence. Cells were plated in duplicate wells, exposed to the 51 candidate compounds for 3 days then allowed to recover in drug-free media for an additional 3 days. After fixing and staining we found cells treated with 24 of the 51 compounds maintained decreased Hoechst 33342 fluorescence less than the average of cells cultured in 25nM Doxorubicin followed by recovery. Visual assessment of these wells confirmed development of SA-β-gal staining and morphology induced by 9 compounds (Figure 5A).

To further reduce the number of candidate compounds we assessed expression of previously established senescence-marker genes *Glb1*(24), *BRAK,* and *Cspg2*(15), in cells exposed to the 9 selected compounds. DU145 cells were treated with 10μM of each compound for 3 days, and RNA isolated was analyzed for gene expression by qPCR. Controls included untreated cells, and cells exposed to idoxyuridine (a compound that induces a quiescent growth arrest). Cells induced to senescence with 25nM Doxorubicin were included as a positive control. Of the candidate compounds, methotrexate, cytarabine, chlorhexidine and IC 261 did not induce significant expression of all three markers (Figure 5B). This experiment was reproduced using the androgen-dependent cell line LNCaP at the 10μM dose (data not shown). All senescent markers were induced in this cell line by 4 of the remaining compounds but not with crassin acetate.

Testing the remaining selected drugs at various concentrations in DU145 cells cultured in 35mm and 100mm plates determined that 250nM AZQ, 10μM Bithionol, 10μM Dichlorophene and 2.5μM Na^+ Pyrithione optimally induce senescence with little apparent cytotoxicity (data not shown). To demonstrate that cells treated with these compounds maintain viability and are not apoptotic, DU145 cells were exposed to the selected compounds for 3 days and assessed for viability and apoptosis by two methods. First, the fraction of viable and apoptotic cells in each culture were assessed by propidium iodide exclusion and Annexin V staining. Cells were cultured in triplicate wells of a 6 well plate, left untreated or exposed to the selected compounds at the above concentrations for 3 days. Cells exposed to 10μM Camptothecin for 6 hr were included as a positive control for apoptosis induction. Cells were then trypsinized, collected, stained with Annexin V and propidium iodide, and analyzed by flow cytometry. Cells exposed to the selected compounds maintained viability in a high percentage of cells, with relatively few apoptotic cells that stain positive with propidium iodide and/or Annexin V (Fig 6A). By contrast, most cells exposed to 10μM Camptothecin for 6 hr stain positive for propidium iodide and/or Annexin V, indicating strong induction of apoptosis. In parallel, cells were cultured in 100mm plates and similarly exposed to candidate compounds for 3 days or 10μM camptothecin for 6 hr, lysed and analyzed for caspase 3 cleavage, a marker of apoptosis. These results show full length caspase 3 in cells exposed to candidate compounds with minimal detection of cleaved caspase 3, similar to untreated cells, while cleaved caspase 3 was easily detected in Campthecin-

treated cells (Fig 6B). These data confirm that DU145 cells exposed to senescence-inducing doses of the candidate compounds for 3 days maintain their viability, with only minor increases in apoptosis induction.

In sum, the initial screen selected 51 compounds (1.2%) out of an original 4160 (Fig 7). Further secondary screens using multiple previously established senescent criteria to reduce the number of candidates lead to 4 final compounds (Table 1). Our data also demonstrates the non-cytotoxic effects of these candidate compounds and validates the ability of our assay to identify senescence-inducing agents.

Discussion

In this study, we describe the development of a rapid screening assay to identify compounds which induce senescence. The induction of senescence has generated significant interest as an approach to prevent cancer cell growth and minimize therapeutic side-effects. Understanding the effects of chemotherapy-induced senescence in human tumors requires the identification and development of specific compounds with this activity in cancer cells. Therefore, novel senescence-inducing compounds are of interest, not only therapeutically, but also to address the mechanistic basis of senescence. To date, efforts to identify agents capable of inducing senescence have largely focused on testing specific compounds to determine the extent to which senescence is induced(12).

The development of methods to detect senescence induction in a high-throughput microscale format presented numerous challenges. The increased

expression of SA-β-gal staining (and its gene *Glb1*) remains a standard marker used to identify senescent cells(5, 6, 24). However, this marker did not significantly change the OD_{600} of whole or solubilized senescent cells when measured using a plate reader (data not shown). Other attempts to utilize engineered cell lines expressing senescence-specific reporter genes (e.g. *cspg2*) were confounded by insignificant induction when proliferating and senescent cells were compared in 96 well plates. Ultimately, we adopted a strategy based on identifying general phenotypic characteristics that define senescent cells. We based the assay primarily on persistent growth arrest in conjunction with increased SA-β-gal staining and changes in morphology.

To approximate assay cell number and detect growth inhibition, we stained cellular nuclei using the fluorescent DNA-binding compound Hoechst 33342. Fluorescently-labeling cells after SA-β-gal staining did not affect the results of either assay (data not shown). This nuclear staining approach generated an acceptable average Z' factor (Z'=0.53 ; Fig 3B) indicating this was a reliable method to reduce the number of candidate compounds from screening libraries. In the pilot library screen, data was analyzed in groups of 384 data points to reduce variation in the data. The average and standard deviation of Hoechst 33342 fluorescence data were calculated, and wells with a decrease in fluorescence of greater than 1 standard deviation were selected for visual assessment (~15% of screened compounds). To add further stringency to this assay we adopted a visual review to quantitate both SA-β-gal staining and senescent morphology. A reliable automated method to assess senescent

morphology and SA-β-gal is not available and represents one area where this technique could be improved. (*Note*: In subsequent screens we have found increasing the stringency for decreased fluorescence more than 2 SD below the average data improved the specificity of the assay.)

Using these criteria, and other confirmatory assays involving persistent growth arrest after drug removal and the expression of known senescence marker genes, our screen identified four structurally and mechanistically diverse compounds from a library of bioactive agents(Table 1). Using methods that molecularly differentiate viable and apoptotic cells, we demonstrate that these drugs produce limited cytotoxicity at effective doses (Fig 6A, 6B). None of these compounds were previously associated with senescence induction. Several of these compounds have demonstrated anti-proliferative activity in cancer cell lines, but have had limited *in vivo* testing. Mechanistically, AZQ is a DNA alkylating compound with limited cytotoxic activity in solid tumor models (25), and the Zn^{2+} ionophore pyrithione induces oxidative stress(26). Both of these cellular stresses are associated with senescence induction(5). The mechanisms by which bithionol and dichlorophene induce senescence remain unknown. The diversity of compounds identified suggests the screen is not biased towards one particular pathway or mechanism.

In summary, we have developed, optimized and validated a novel high-throughput assay to screen chemical libraries for senescence-inducing compounds. It is a rapid technique that utilizes detection methods commonly found in most laboratories. Utilizing the methods and criteria outlined in the

project, we were able to identify a unique group of compounds that are capable of inducing senescence. These agents provide a basis for further studies into the therapeutic induction of senescence in tumor cells *in vitro* and *in vivo*. Finally, these compounds will facilitate the investigation of molecular pathways regulating the senescence response in cancer cells.

Figure Legends

Figure 1. Senescent morphology and SA-β-gal activity. Phase contrast microscopy of DU145 cells cultured -/+ 250nM AZQ for 3 days. Senescent cells become enlarged and flattened with a "fried egg" appearance and blue SA-β-gal staining. Original image magnification: 400x.

Figure 2: Screen for the identification of senescence in cancer cells. Prostate cancer cell lines were exposed to a library of compounds for 3 days, fixed and stained overnight for SA-β-gal activity, followed by staining with Hoechst 33342. Compounds of interest were initially identified by decreased Hoechst 33342 fluorescence indicating senescence or apoptosis. Then, candidate wells were visually assessed to identify the presence of SA-β-gal activity and senescent morphology.

Figure 3. Development of Hoechst 33342 fluorescence to differentiate senescence in treated cancer cells. **A.** DU145 cells were cultured in a 96-well plate treated with increasing doses of Doxorubicin (n=14). Previous studies have demonstrated 25nM to induce senescence and over 100nM to induce apoptosis[ref]. Cells were cultured three days, fixed, stained for SA-β-gal activity and Hoechst 33342. Blank wells were included as negative controls. **B.** Calculation of Z' in senescent versus proliferating DU145 cells. Cells were cultured -/+25nM Doxorubicin for 3 days before being stained and Hoechst

33342 fluorescence measured by plate reader. The average Z' of all four experiments was 0.53 (students t-test: $p<0.003$). Error bars represent one standard error.

Figure 4. Fluorescence data from screen of known bioactive compound library. Hoechst 33342 fluorescence measured in cells treated with library compounds or DMSO as a vehicle. Fluorescence data was analyzed in groups of 384 data points to reduce variation, and the average and standard deviation was calculated for each group. Wells with fluorescence more than 1 SD below the average of all data (open circles) were selected to be visually assessed for SA-β-gal activity and senescence morphology.

Figure 5. Confirmatory assays for senescence. **A.** Persistence of proliferative arrest after drug removal. Wells with Hoechst 33342 fluorescence lower than the average of DOX-treated cells (open circles) were visually inspected, identifying 9 compounds that maintained senescence (X over open circle). All data are averages of duplicates.

B. Expression of senescence marker genes *Glb1, BRAK* and *Cspg2* in DU145 cells treated with 9 candidate compounds versus untreated. In triplicate wells, RNA was harvested and qPCR performed and results normalized to *18S* expression and then untreated cells. Cells were exposed to 10μM idoxyuridine,

which induces quiescence, as a negative control (* signifies selection for further investigation). These results are representative of two independent experiments.

Figure 6. Cell viability and apoptosis in DU145 cells treated with final selected compounds. Error bars represent standard error. **A.** Propidium iodide exclusion/Annexin V staining was used to identify viable and apoptotic cells. Cells treated with Camptothecin are included as a control. These results are representative of two independent experiments. **B.** Immunoblot analysis of full length and cleaved caspase 3 in lysates of treated cells, including Camptothecin as a control. These results are representative of two independent experiments.

Figure 7. Flow diagram of screening methods and results of pilot library screening. The initial screen identified 51 candidate that were further selected by secondary assays, identifying four final compounds.

Table 1: Senescence-inducing compounds identified by high throughput screening. Results of *in vitro* and *in vivo* anti-cancer screens deposited in PubChem and reported mechanisms targeted by each compound. Structures of identified compounds (left to right): AZQ; Bithionol; Pyrithione; Dichlorophene.

Fig 1

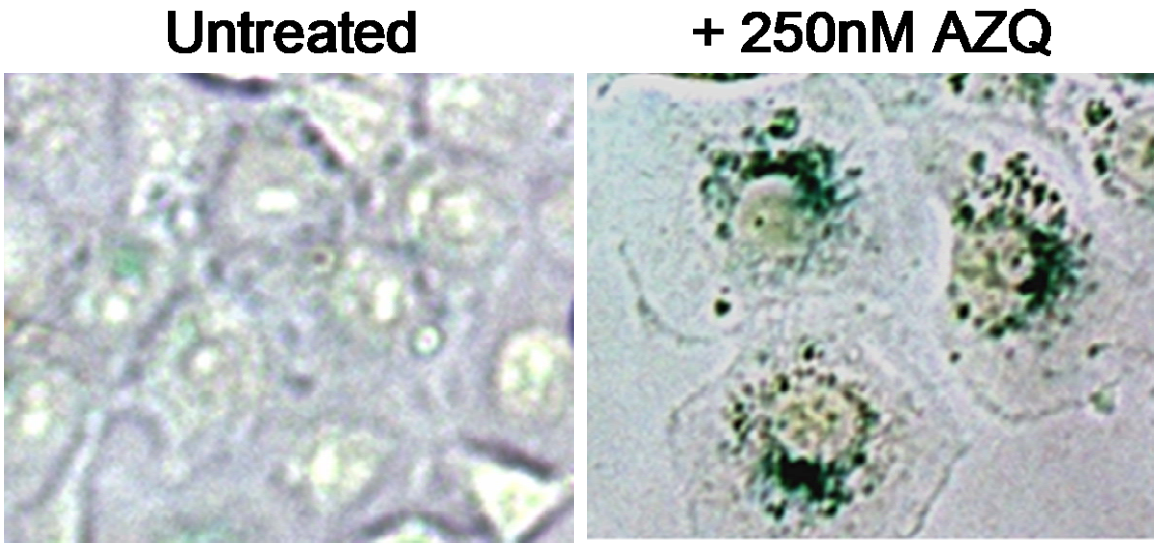

Fig 2

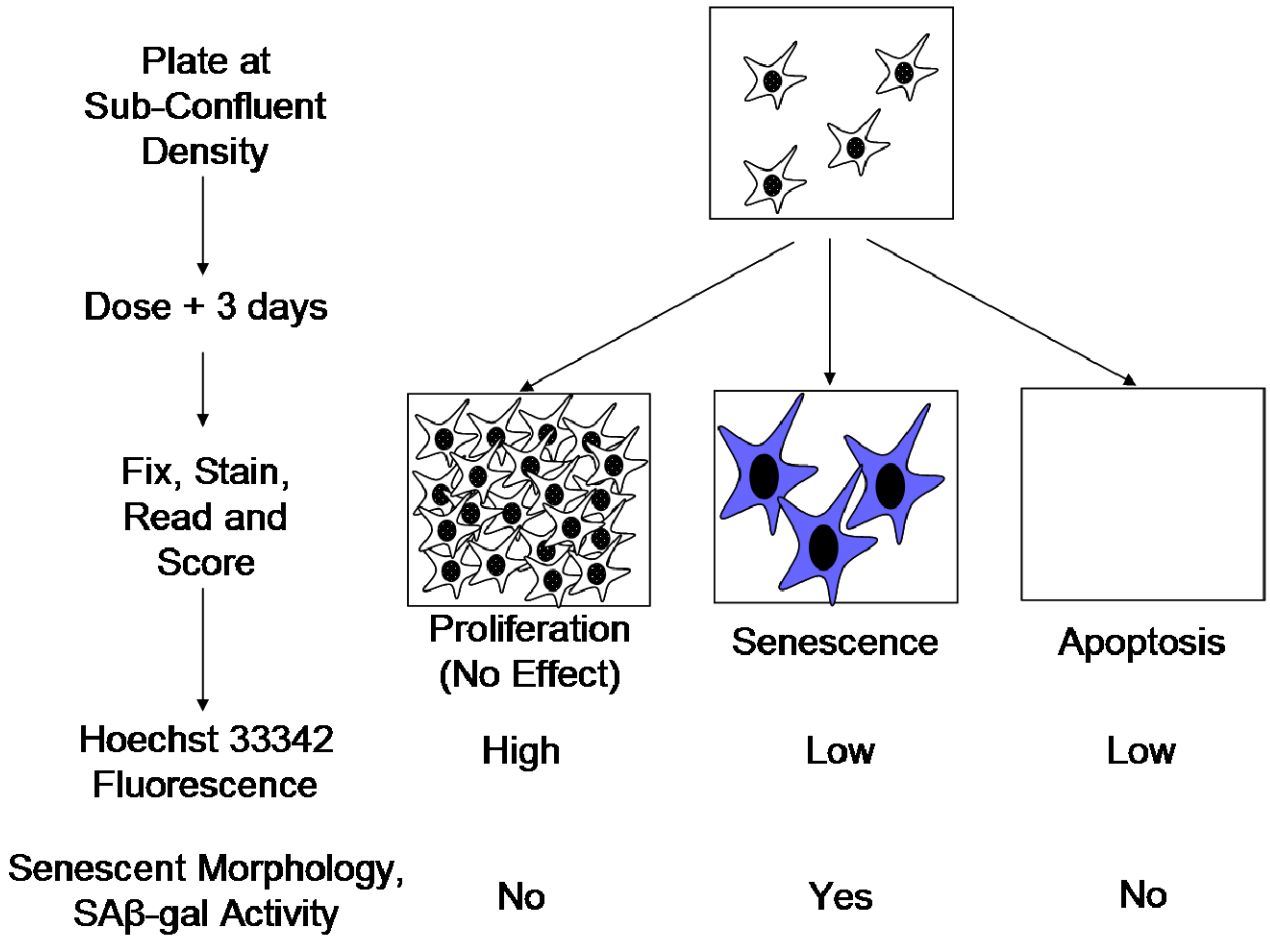
Plate at Sub-Confluent Density
Dose + 3 days
Fix, Stain, Read and Score
Proliferation (No Effect)
Senescence
Apoptosis
Hoechst 33342 Fluorescence
High
Low
Low
Senescent Morphology, SAβ-gal Activity
No
Yes
No

Fig 3

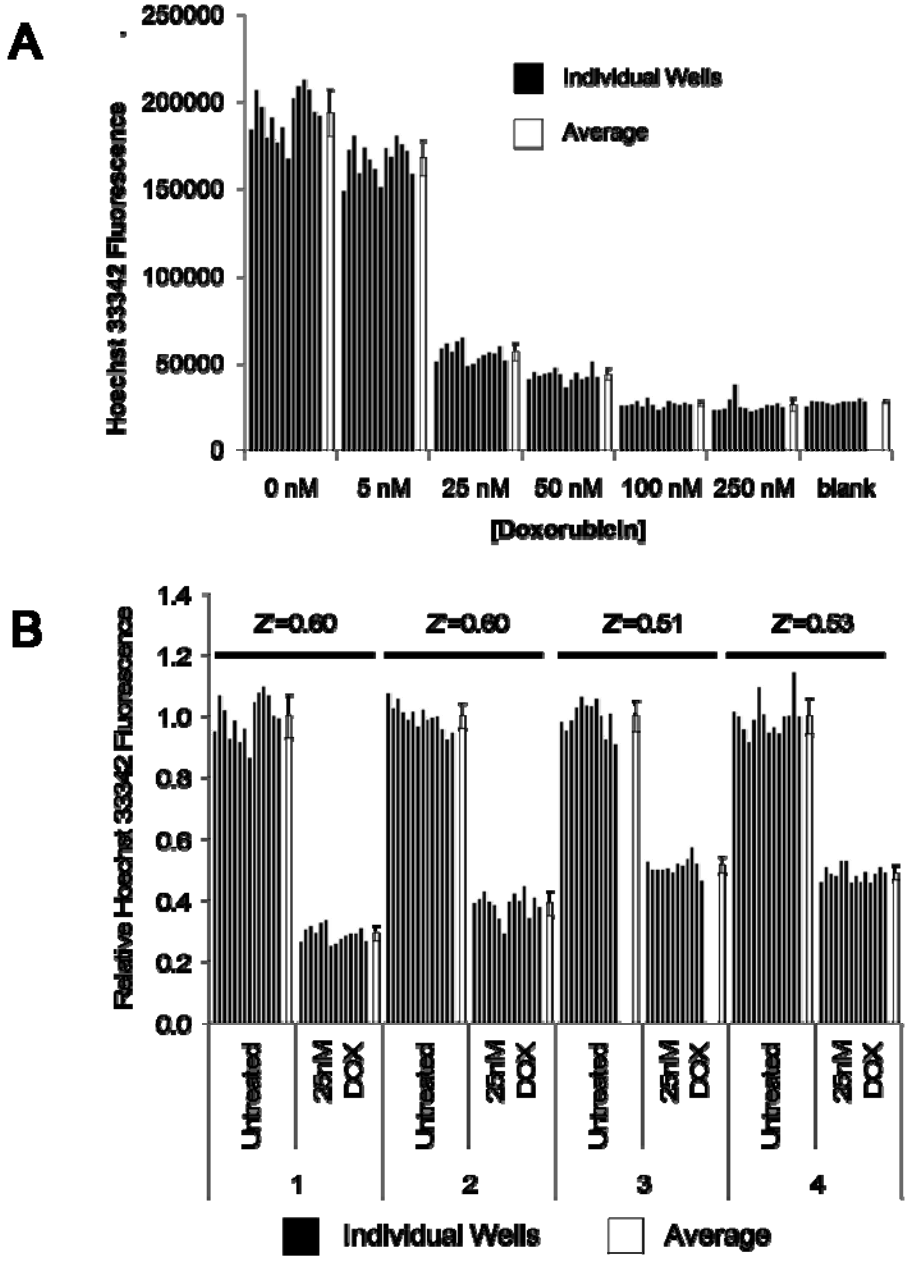
A
250000
200000
150000
100000
50000
0
Hoechst 33342 Fluorescence
Individual Wells
Average
0 nM
5 nM
25 nM
50 nM
100 nM
250 nM
blank
[Doxorubicin]
B
1.4
1.2
1.0
0.8
0.6
0.4
0.2
0.0
Relative Hoechst 33342 Fluorescence
Z'=0.60
Z'=0.60
Z'=0.51
Z'=0.53
Untreated
25nM DOX
1
2
3
4
Individual Wells
Average

Fig 4

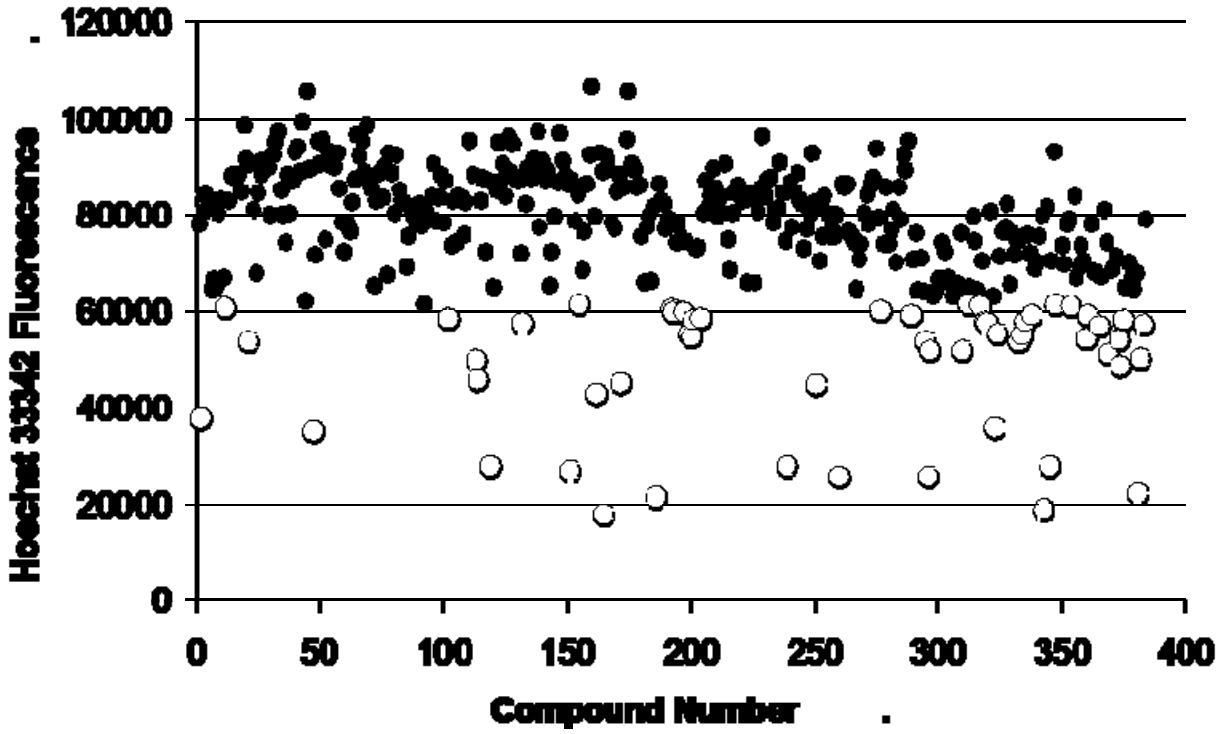
Hoechst 33342 Fluorescence
120000
100000
80000
60000
40000
20000
0
0
50
100
150
200
250
300
350
400
Compound Number

Fig 5

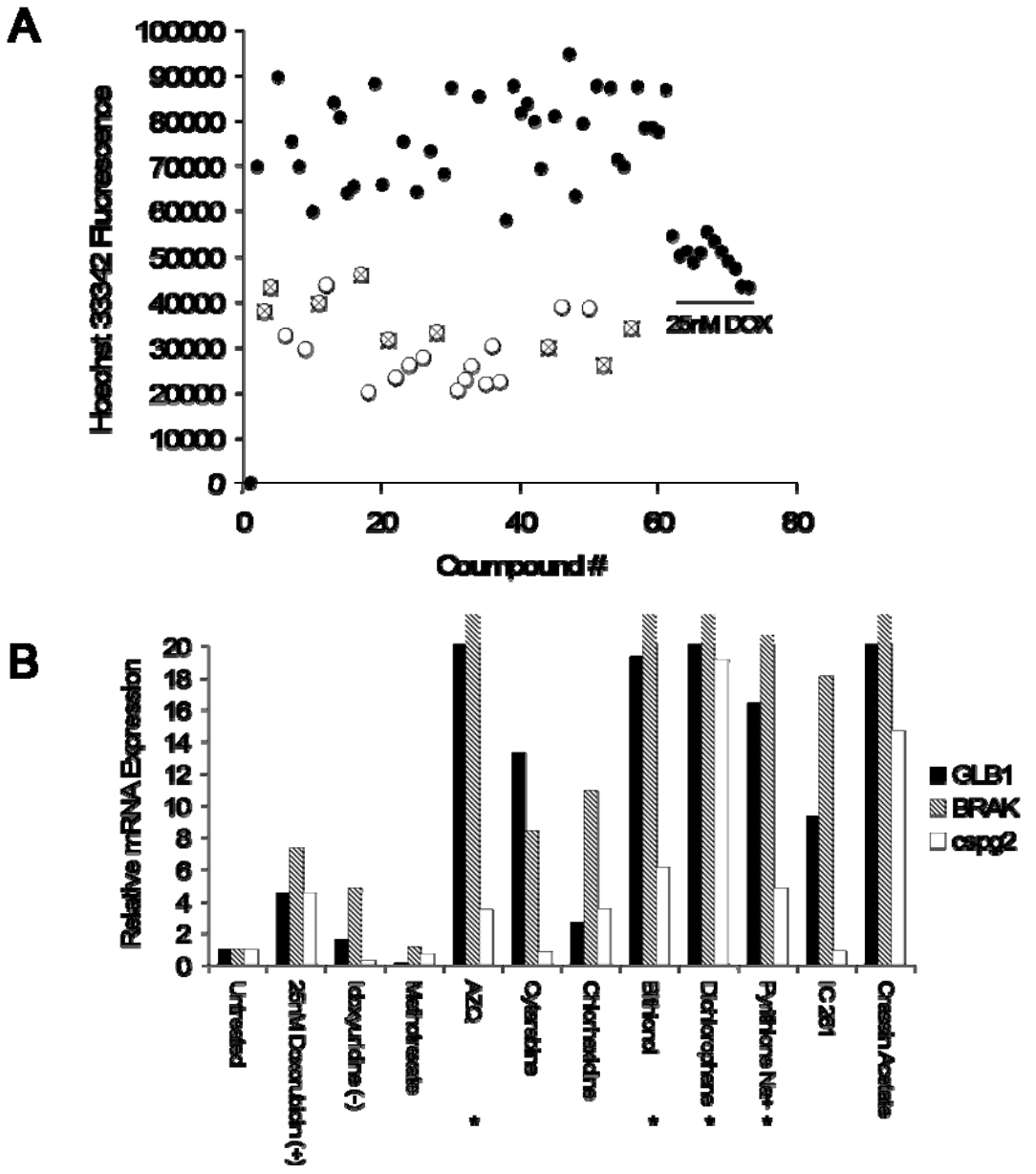
A
Hoechst 33342 Fluorescence
100000
90000
80000
70000
60000
50000
40000
30000
20000
10000
0
0
20
40
60
80
Compound #
25nM DOX
B
Relative mRNA Expression
20
18
16
14
12
10
8
6
4
2
0
GLB1
BRAK
cspg2
Untreated
25nM Doxorubicin (+)
Idoxuridine (-)
Mafenidesate
AZQ
Cytarabine
Chlorhexidine
Etifibrol
Dichlorophene
Pyrithione Na+
IC 261
Crassin Acetate
*
*
*
*

Fig 6

A

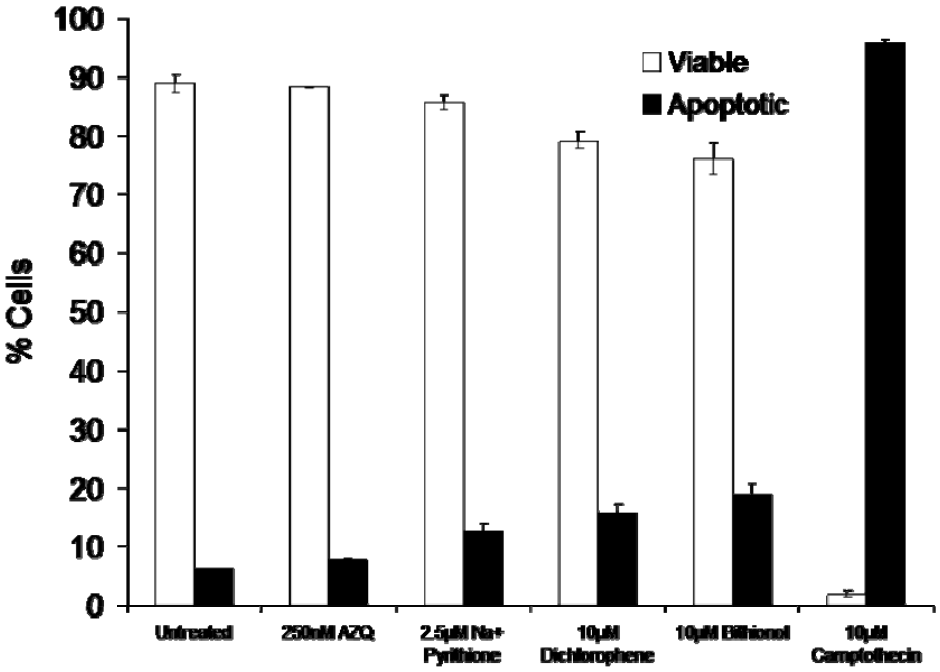

B

Data Pending

Fig 7

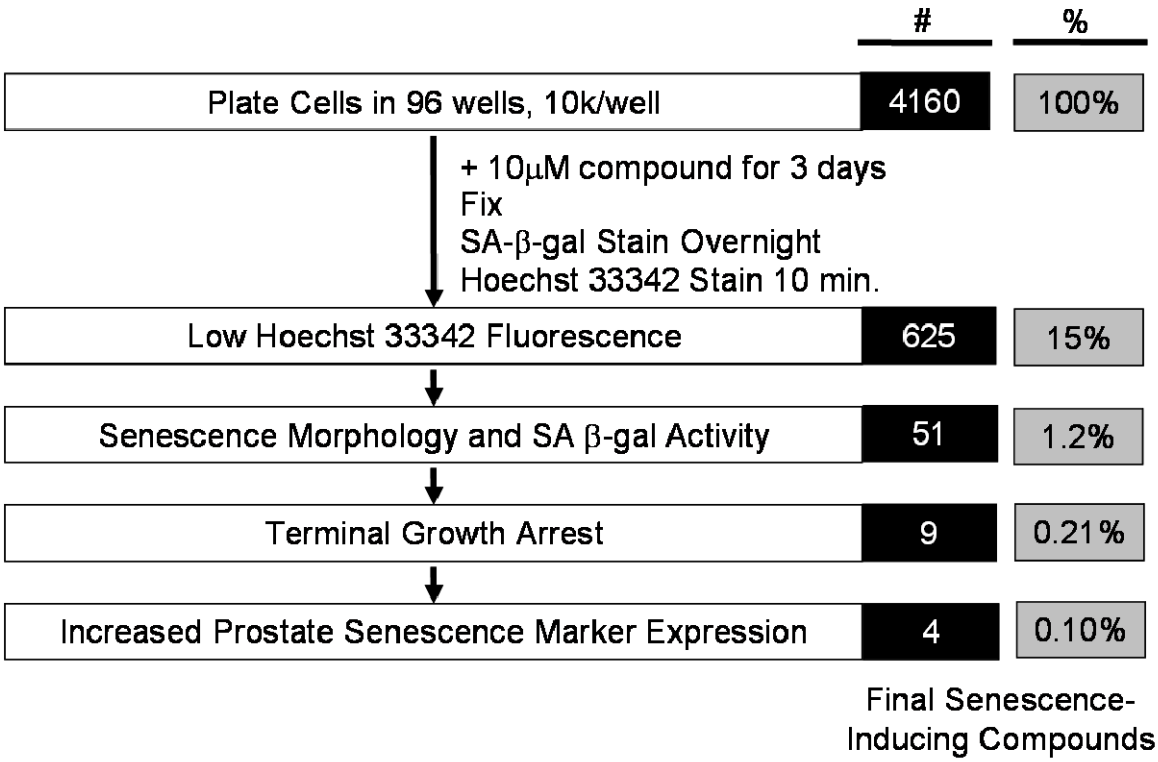
#
%
Plate Cells in 96 wells, 10k/well
4160
100%
+ 10μM compound for 3 days
Fix
SA-β-gal Stain Overnight
Hoechst 33342 Stain 10 min.
Low Hoechst 33342 Fluorescence
625
15%
Senescence Morphology and SA β-gal Activity
51
1.2%
Terminal Growth Arrest
9
0.21%
Increased Prostate Senescence Marker Expression
4
0.10%
Final Senescence-Inducing Compounds

Table 1

Compound	PubChem ID	PubChem: Anti-Cancer Activity		Reported Mechanism of Action
		in vitro	*in vivo*	
AZQ	42616	+	-	DNA Alkylating
Bithionol	2406	+	-	N/A
Pyrithione	1570	+	N/A	Zn^{2+} Ionophore
Dichlorophene	3037	+	-	N/A

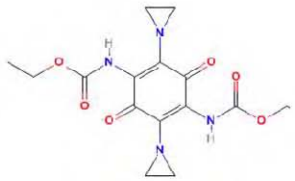

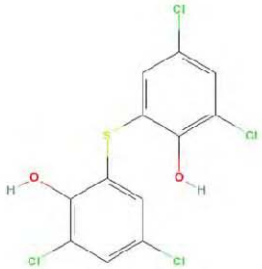

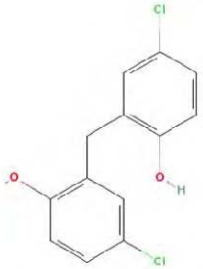

Literature Cited

1. Winquist, E, Waldron, T, Berry, S, Ernst, DS, Hotte, S, and Lukka, H Non-hormonal systemic therapy in men with hormone-refractory prostate cancer and metastases: a systematic review from the Cancer Care Ontario Program in Evidence-based Care's Genitourinary Cancer Disease Site Group. BMC Cancer, 2006; *6*(112.
2. Roninson, IB Tumor cell senescence in cancer treatment. Cancer Res, 2003; *63*(11)*:* 2705-2715.
3. Schmitt, CA Cellular senescence and cancer treatment. Biochim Biophys Acta, 2007; *1775*(1)*:* 5-20.
4. Ben-Porath, I and Weinberg, RA When cells get stressed: an integrative view of cellular senescence. J Clin Invest, 2004; *113*(1)*:* 8-13.
5. Campisi, J and d'Adda di Fagagna, F Cellular senescence: when bad things happen to good cells. Nat Rev Mol Cell Biol, 2007; *8*(9)*:* 729-740.
6. Dimri, GP, Lee, X, Basile, G, *et al.* A biomarker that identifies senescent human cells in culture and in aging skin in vivo. Proc Natl Acad Sci U S A, 1995; *92*(20)*:* 9363-9367.
7. Ben-Porath, I and Weinberg, RA The signals and pathways activating cellular senescence. Int J Biochem Cell Biol, 2005; *37*(5)*:* 961-976.
8. Collado, M, Gil, J, Efeyan, A, *et al.* Tumour biology: senescence in premalignant tumours. Nature, 2005; *436*(7051)*:* 642.
9. Denoyelle, C, Abou-Rjaily, G, Bezrookove, V, *et al.* Anti-oncogenic role of the endoplasmic reticulum differentially activated by mutations in the MAPK pathway. Nat Cell Biol, 2006; *8*(10)*:* 1053-1063.
10. Michaloglou, C, Vredeveld, LC, Soengas, MS, *et al.* BRAFE600-associated senescence-like cell cycle arrest of human naevi. Nature, 2005; *436*(7051)*:* 720-724.
11. Majumder, PK, Grisanzio, C, O'Connell, F, *et al.* A prostatic intraepithelial neoplasia-dependent p27 Kip1 checkpoint induces senescence and inhibits cell proliferation and cancer progression. Cancer Cell, 2008; *14*(2)*:* 146-155.
12. Chang, BD, Broude, EV, Dokmanovic, M, *et al.* A senescence-like phenotype distinguishes tumor cells that undergo terminal proliferation arrest after exposure to anticancer agents. Cancer Res, 1999; *59*(15)*:* 3761-3767.
13. Chang, BD, Swift, ME, Shen, M, Fang, J, Broude, EV, and Roninson, IB Molecular determinants of terminal growth arrest induced in tumor cells by a chemotherapeutic agent. Proc Natl Acad Sci U S A, 2002; *99*(1)*:* 389-394.
14. Roberson, RS, Kussick, SJ, Vallieres, E, Chen, SY, and Wu, DY Escape from therapy-induced accelerated cellular senescence in p53-null lung cancer cells and in human lung cancers. Cancer Res, 2005; *65*(7)*:* 2795-2803.
15. Schwarze, SR, Fu, VX, Desotelle, JA, Kenowski, ML, and Jarrard, DF The identification of senescence-specific genes during the induction of senescence in prostate cancer cells. Neoplasia, 2005; *7*(9)*:* 816-823.

16. te Poele, RH, Okorokov, AL, Jardine, L, Cummings, J, and Joel, SP DNA damage is able to induce senescence in tumor cells in vitro and in vivo. Cancer Res, 2002; *62*(6)*:* 1876-1883.
17. Petti, C, Molla, A, Vegetti, C, Ferrone, S, Anichini, A, and Sensi, M Coexpression of NRASQ61R and BRAFV600E in human melanoma cells activates senescence and increases susceptibility to cell-mediated cytotoxicity. Cancer Res, 2006; *66*(13)*:* 6503-6511.
18. Schmitt, CA, Fridman, JS, Yang, M, *et al.* A senescence program controlled by p53 and p16INK4a contributes to the outcome of cancer therapy. Cell, 2002; *109*(3)*:* 335-346.
19. Xue, W, Zender, L, Miething, C, *et al.* Senescence and tumour clearance is triggered by p53 restoration in murine liver carcinomas. Nature, 2007; *445*(7128)*:* 656-660.
20. Zhang, JH, Chung, TD, and Oldenburg, KR A Simple Statistical Parameter for Use in Evaluation and Validation of High Throughput Screening Assays. J Biomol Screen, 1999; *4*(2)*:* 67-73.
21. Ewald, JA, Desotelle, JA, Almassi, N, and Jarrard, DF Drug-induced senescence bystander proliferation in prostate cancer cells in vitro and in vivo. Br J Cancer, 2008; *98*(7)*:* 1244-1249.
22. Ewald, JA, Wilkinson, JC, Guyer, CA, and Staros, JV Ligand- and kinase activity-independent cell survival mediated by the epidermal growth factor receptor expressed in 32D cells. Exp Cell Res, 2003; *282*(2)*:* 121-131.
23. Isaacs, WB, Carter, BS, and Ewing, CM Wild-type p53 suppresses growth of human prostate cancer cells containing mutant p53 alleles. Cancer Res, 1991; *51*(17)*:* 4716-4720.
24. Lee, BY, Han, JA, Im, JS, *et al.* Senescence-associated beta-galactosidase is lysosomal beta-galactosidase. Aging Cell, 2006; *5*(2)*:* 187-195.
25. Bender, JF, Grillo-Lopez, AJ, and Posada, JG, Jr. Diaziquone (AZQ). Invest New Drugs, 1983; *1*(1)*:* 71-84.
26. Seo, SR, Chong, SA, Lee, SI, *et al.* Zn2+-induced ERK activation mediated by reactive oxygen species causes cell death in differentiated PC12 cells. J Neurochem, 2001; *78*(3)*:* 600-610.